University of Alberta

Oxygen is required to retain Ero1α on the MAM

by

Susanna Yael Gilady

A thesis submitted to the Faculty of Graduate Studies and Research
in partial fulfillment of the requirements for the degree of

Master of Science

Department of Cell Biology

Fall 2009
Edmonton, Alberta

Examining Committee

Dr. Thomas Simmen, Department of Cell Biology, University of Alberta

Dr. Gary Eitzen, Department of Cell Biology, University of Alberta

Dr. Shairaz Baksh, Department of Pediatrics, University of Alberta

Dedication

To all the great kids from the Stollery Children's Hospital.

Your smiles and extraordinary strength will never be forgotten.

Abstract

Oxidative protein folding within the ER depends on the enzymatic action of numerous chaperones and oxidoreductases. In addition, this process requires the influx of metabolites and energy, including FAD (flavin adenine dinucleotide) and molecular oxygen. Secretory proteins and proteins destined to the secretory pathway need to undergo this process in order to obtain stability and full functionality. Since secretory proteins that fail to fully fold are eliminated by degradation, the process of ER oxidative protein folding is part of a group of ER-associated mechanisms commonly referred to as ER quality control. Interestingly, the proteins that mediate ER quality control can be found in a variety of diverse subdomains of the ER. We have found that the ER-oxidoreductase Ero1α is located on the mitochondria-associated-membrane, the MAM. This specialized subdomain of the ER has been shown to be crucial for a number of processes such as the synthesis of phospholipids as well as calcium-channelling between the ER and mitochondria. The goal of this thesis was to identify possible retention mechanisms and motifs of Ero1α to the MAM.

Acknowledgements

First and foremost, I would like to thank my husband, best friend and soul mate, Erez Gilady, for all his support and love throughout the years. I really don't know what I would do without you! Love you lots!

I would like to thank my parents for everything they have done for me and for raising me to be the person that I am today. My deepest gratitude to Eva, who has been very important to me in many aspects of my life...as a parent, an aunt, a good friend, an advisor and a great supporter. Always! I am very thankful for having such great parents-in-law! Sima and Gideon have been so supportive for the past years. It is beyond all words. Thank you for accepting me for the way I am and for acknowledging me as part of your family as if I was your own daughter! Of course I would like to thank all the other family members, whose names I have not mentioned here.

As far as research is concerned, I would like to thank my supervisor, Dr. Thomas Simmen for taking me into his lab and for all his research-expertise. I would like to thank my committee members, Drs. Gary Eitzen, Marek Michalak, Paul Melancon and Shairaz Baksh; as well as all the past and present lab members of the Simmen lab.

A special "thank you" to Carolina, Dale, Ava, Nathan, Maneka and Mike for critically reading this thesis. Thank you for jumping in and helping me out.

I would particularly like to thank Maneka and Dale for all their support when it came to practising talks/presentations throughout the last 2 years. You guys were a great help. A big thank you to Susan! You have been a great and true friend to me! I know that I can always count on you. I will sincerely miss our 'early-morning-chats'. As a 'half-lab-member', I would like to thank Ava. I am very glad that we got to spend some time together in the lab and got to know each other! Too bad, it was so short, though. And what would the past two years of lab

meetings been like without the Goping-gang?! I can't even imagine. Thank you for the great and fun lab meetings we have had together!

I would like to thank Claire, Kendall and Nikki for all their help! My year as the president of CBSA would have been so much harder if it wasn't for Colleen. Thank you so much for all your help! Deborah Giles: some people might think she is just the 'Student Program Secretary' but she is so much more. I would like to express my gratitude to you for everything you have done for me! Your door has always been open for me. Thank you for all your support and help; and most importantly: for always listening when I needed someone to talk to!

Dr. Tom Hobman, thank you so much for helping me find my new path!

Last but not least, I would like to thank my new supervisor, Dr. Andrew Mason, for taking me into his lab. I look forward to many years of exciting research!

Table of Contents

List of Figures

List of Abbreviations

ADP	Adenosine diphosphate
AMFR	Autocrine motility factor receptor
ATF4	Activating transcription factor 4
ATF6	Activating transcription factor 6
ATP	Adenosine triphosphate
BAX	Bcl-2-associated X protein
BAK	Bcl-2 homologous antagonist killer
BCL-2	B-cell lymphoma family
BiP	Binding immunoglobulin protein
bZIP	Basic leucine zipper domain
Ca^{2+}	Calcium
CHOP	CCAAT/enhancer binding protein
CNX	Calnexin
CRT	Calreticulin
ddH_2O	Double distilled water
DTT	Dithiothreitol
e^-	Electron
EDEM	ER degradation enhancing-mannosidase-like protein
EF	Helix-loop-helix structural domain (for Calcium binding)
eIF2α	Eukaryotic translation initiation factor 2A
EPO	Erythropoietin
ERAD	ER-associated degradation
ER	Endoplasmic reticulum
ERGIC	ER-Golgi-intermediate compartment
ERMan1	ER-mannosidase 1

Ero1	ERoxidoreductase
ERSE	ER-stress response element
FAD	Flavin adenine dinucleotide
GAPDH	Glyceraldehyde 3-phosphate dehydrogenase
Glc	Glucose
Grp	Glucose-regulated protein
Grp78	Glucose-regulated-protein 78 (BiP)
HEK293T	Human embryonic kidney cells
HeLa	Cervical cancer cell line (Henrietta Lacks)
HIF	Hypoxia-inducible-factor
HO-1	Heme oxygenase 1
HRE	Hypoxia response element
Hsp70	Heat-shock-protein 70
i-NOS	Calcium-insensitive nitric oxide synthase
IP_3R1	Inositol triphosphate receptor type 1
IRE1	Inositol-requiring enzyme 1
JNK	c-Jun N-terminal kinase
kDa	kilo Dalton
KDEL	Amino acid sequence: Lys-Asp-Glu-Leu
MAM	Mitochondria-associated-membrane
MEF	Mouse embryonic fibroblasts
mRNA	Messenger ribonucleic acid
O_2	Molecular oxygen
PDI	Protein disulfide isomerase
PDILT	A specific protein disulfide isomerase
PERK	Phosphorylated ERK (extracellular signal-regulated kinase)
pVHL	Von Hippel-Landau tumor suppressor protein

SDS-PAGE	Sodium dodecyl sulphate polyacrylamide gel electrophoresis
SERCA	Sarco/endoplasmic reticulum Ca^{2+} ATPase
Sig-1R	Sigma 1 receptor
SRP	Signal recognition particle
TCA	Trichloroacetic acid
TCA cycle	Tricarboxylic acid cycle (Krebs cycle)
Rcf	Relative centrifugal force
rER	rough ER
sER	smooth ER
RIP	Regulated intramembrane proteolysis
UDP	Uridine diphosphate
UGGT	(UDP)-glucose: glycoprotein glucosyltransferase
UPR	Unfolded protein response
VDAC	Voltage dependent anion channel
VEGF	Vascular endothelial growth factor
VIPL	VIP36-Like membrane protein
Xbp1	X-box binding protein 1
Zn^{+}	Zinc
2ME	β-mercaptoethanol

Chapter 1 – Introduction

1.1 Oxidative Protein Folding

Initially, proteins result from the translation of mRNA at ribosomes into amino acid chains (Brenner *et al.* 1961). These amino acid chains are non-functional linear polypeptide chains. Only their folding activates their characteristics and functionality (Seckler and Jaenicke 1992). The process of protein folding involves two main steps: first, the synthesis of polypeptides on ribosomes and secondly, accurate folding to allow for proper functioning of the protein. Unlike so many processes within the cell, protein folding in eukaryotes is required to occur in two cellular compartments with very different chemical environments, the cytosol and the endoplasmic reticulum (ER) (Riemer *et al.* 2009). Whereas the ER provides an oxidizing environment that facilitates the formation of disulfide bonds, the cytosol tends to be reducing. Nascent polypeptides that are destined to enter the secretory pathway enter the endoplasmic reticulum at the translocon, which recognizes signal sequences. Once the nascent polypeptide has successfully been translocated into the ER lumen, the oxidative protein folding begins.

Most proteins inserted into the ER require the action of ER chaperones to become fully folded and functional (Kramer *et al.* 2009). The majority of these proteins are destined to be secreted or to be exposed on the cell surface. The lack of a chaperone-machinery on the cell surface makes it inevitable for these proteins to be folded precisely and obtain exceptional stability before they leave the ER (Bardwell 2004; Riemer *et al.* 2009). It is estimated that about 20% of all proteins

in humans actually contain disulfide bonds (Lees 2008). Disulfide bonds are formed by the pair-wise oxidation of cysteine residues to give a scaffold-like structure to the unfolded protein (Lees 2008). Oxidative protein folding comprises of three different processes: The thiol-groups of a protein can be oxidized to form disulfides (-S-S-), disulfide bonds can be reduced to thiols (-S-H H-S-), or existing disulfide bonds that are in a non-native state, can be re-arranged to allow for proper protein folding into a native state, referred to as isomerization (Lees 2008).

Anfinsen and colleagues had discovered 40 years ago that oxidative protein folding or rather the formation of native disulfide bonds was a spontaneous event. However, *in vitro* versus *in vivo* experiments showed that the formation of these disulfide bonds seemed to happen much faster in living cells (Frand *et al.* 2000). This finding suggested that some sort of enzymatic catalyst was involved in the proper folding of proteins (Frand *et al.* 2000). This central enzyme, mediating the formation of disulfide bonds, is the thiol oxidoreductase protein disulfide isomerase (PDI) (Ellgaard and Ruddock 2005). PDI oxidizes newly synthesized proteins that enter the ER by forming and isomerising disulfide bonds (Tu and Weissman 2004). There are a total of 17 disulfide isomerases found in the mammalian ER (Maattanen *et al.* 2006). The first thioredoxin family protein to be discovered was PDI and its characterization led to the finding that it contains four thioredoxin-like domains (Goldberger *et al.* 1964). The first a domain as well as the last a' domain contain catalytic CXXC-motifs whereas the middle two domains are non-catalytic (Gruber *et al.* 2006). Between those two

cysteine residues are two amino acids situated that are the main criteria in determining the redox potential of the enzyme and its functional capability (Ellgaard and Ruddock 2005). These amino acid residues with their specific characteristics can thus control the pK_a of the two cysteines that are part of the active motif (Ellgaard and Ruddock 2005). Moreover, apart from PDI's function in disulfide bond formation, it has been shown to bind to calcium, thus regulating ER-calcium-homeostasis together with other calcium binding proteins within the ER (Corbett *et al.* 1999).

There are three other protein disulfide isomerases that share this very same motif-structure: ERp57, PDIp, and PDILT. Another protein disulfide isomerase is ERp72 which contains an additional catalytic a domain (Hatahet and Ruddock 2007). All these protein disulfide isomerases are listed with their structures in Figure 1.1. Given that there are 17 protein disulfide isomerases, the question arises as to why there are so many different ones. There are no conserved substrate-binding-sites found among all the PDIs, the non-catalytic domains vary while the catalytic domains are conserved but show variations in their redox-active motifs (Maattanen *et al.* 2006). One possibility for this large number of PDIs could be that it allows for numerous protein-protein interactions. For a number of years, it remained unknown how PDI would get re-oxidized (Freedman *et al.* 1998). However, it was later discovered in yeast that Ero1p was the missing link in this puzzle (Figure 1.2) (Frand and Kaiser 1998; Pollard *et al.* 1998). In yeast, PDI directly receives disulfide bonds from the oxidoreductase Ero1p (endoplasmic reticulum oxidoreductase1) which is located in the ER lumen. This

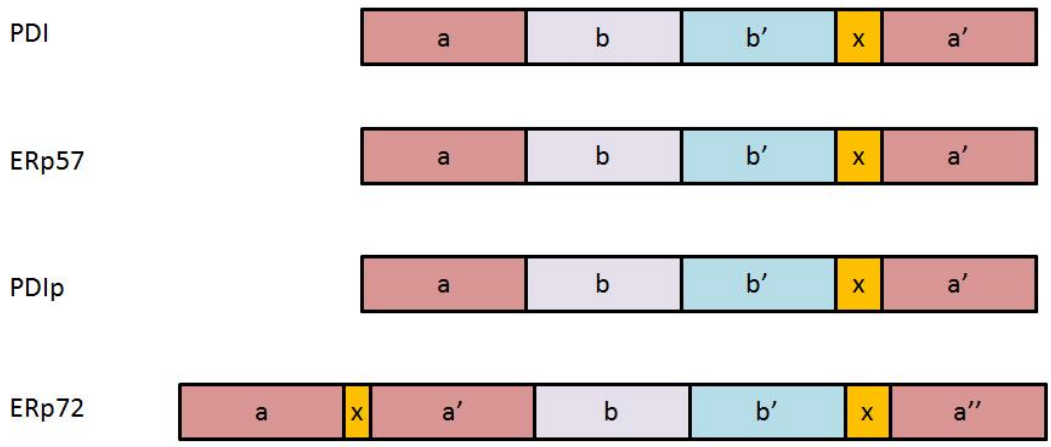

Figure 1.1: Protein disulfide isomerases. The schematic shows the eukaryotic protein isomerases PDI, ERp57, PDIp and ERp57. All of which contain the regulatory domains indicated by the letter 'a' and non-catalytic domains ('b'). Linker domains are represented by an 'x'. (Modified from Maattanen *et al.*, Biochem Cell Biol. 2006)

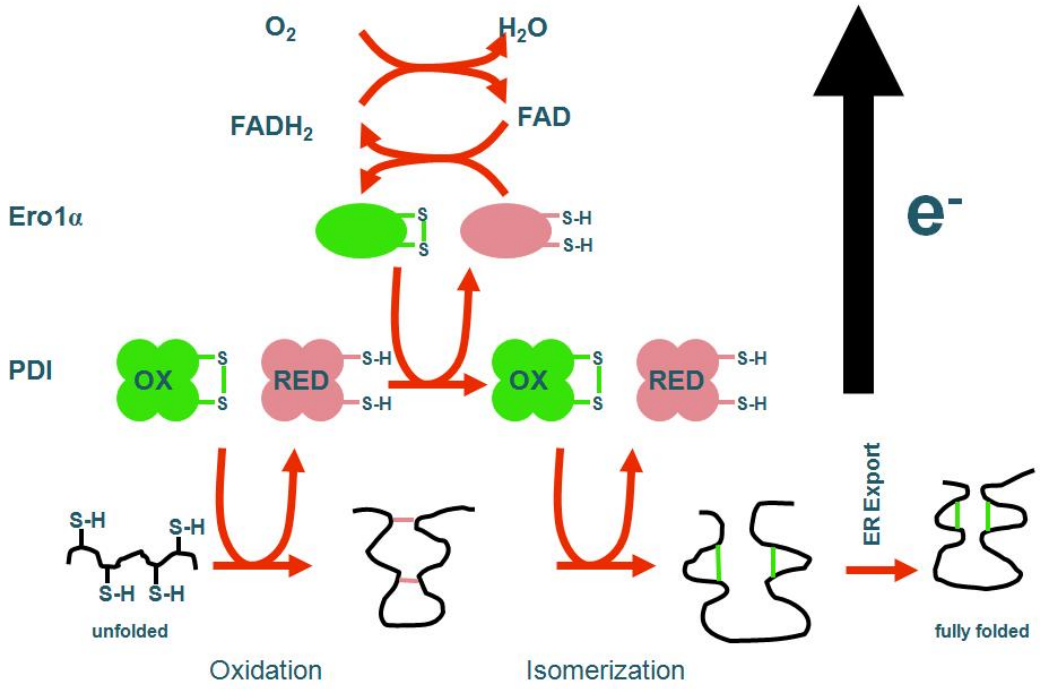

Figure 1.2: Oxidative protein folding. The schematic shows all key molecular components involved in Ero1/PDI oxidative protein folding. This whole process represents an electron transport chain starting with the unfolded protein that gets oxidized by PDI (protein disulfide isomerase), then onto Ero1α to FAD (flavin adenine dinucleotide) with the terminal electron acceptor as molecular oxygen.

is accomplished by direct interactions via the formation of mixed disulfides between the two proteins. The flavoprotein Ero1 is FAD-dependent for it receives the electrons that are then handed over to molecular oxygen (Dias-Gunasekara *et al.* 2006). The transfer of the disulfide bonds from Ero1 to PDI and from FAD to Ero1 occurs at the redox active sites (Tu and Weissman 2002).

After the discovery of Ero1α in yeast, the search for human homologues led to two proteins, identified in humans and mice: Ero1α and –β (Cabibbo *et al.* 2000; Pagani *et al.* 2000). A comparison of these two proteins with yeast ortholog revealed that both Ero1α and β lack a sequence of about 127 amino acids at the C-terminus. This specific 'tail' was found to be essential for Ero1p to bind to the membrane of the ER (Pagani *et al.* 2001).

The ER oxidoreductases α and β both reside in the lumen of the ER and are found to be upregulated upon ER stress (Gess *et al.* 2003). Under resting conditions, expression levels of Ero1α can be easily detected whereas the other isoform, Ero1β, seems to be only measurable in specified tissues such as the pancreas or upon ER stress (Pagani *et al.* 2000). Pancreatic cells are professional insulin producing cells which means that large amounts of secretory proteins have to be folded here. Ero1α but not β has been found to be a direct transcriptional target of the hypoxia-inducible-factor-1 (HIF1), consequently making Ero1α an oxygen regulated gene (Gess *et al.* 2003). In addition, there are two isoforms of Ero1α (OX1 and OX2) that have been shown to denote the oxidized redox state of Ero1α (Appenzeller-Herzog *et al.* 2008). OX1 and OX2 are detectable on non-

reducing gels where OX2 has been shown to migrate faster than OX1. This was first described by Anelli *et al* (2002) and led essentially to the finding that OX2 was comprised of a long-ranged disulfide bond between the cysteine residues C94 and C131 (Appenzeller-Herzog *et al.* 2008). Subsequent analysis of OX2 mutants revealed a functional requirement of OX2 for the redox homeostasis within the ER. These findings were discovered by Appenzeller-Herzog *et al* (2008).

There are certain structural and functional differences when comparing Ero1α and –β. Both Ero1α and –β have a signal sequence at the N-terminus which targets these two to the endoplasmic reticulum (Dias-Gunasekara and Benham 2005). Ero1α shows two glycosylation sites, whereas Ero1β has four of them. It is unknown, if the number of glycosylation sites result in functional differences. Ero1α and –β both have two conserved redox-motifs: CXXXXC near the N-terminus and CXXCXXC near the C-terminus (Figure 1.3). The first of the two active sites motif is involved in exchanging disulfide bonds with PDI (CXXXXC) and also accepts the electrons as part of the electron transport chain (Figure 1.2). These electrons are transferred to the second active site where the second and third cysteines of CXXCXXC are then responsible for passing the electrons to FAD and then to the terminal electron acceptor, O_2. Conversely, it has been shown in yeast that an alternative electron acceptor does exist, which is fumarate (Bader *et al.* 1999). It is likely that there is also an alternative electron acceptor to molecular oxygen in mammalians but its identity remains unknown. Using molecular oxygen as the terminal electron acceptor however, has severe consequences for the cell. It has been proposed that oxidative protein folding

involving Ero1α might produce reactive oxygen species (ROS) which could add to the overall cellular oxygen stress level within the cell (Tu and Weissman 2004).

Ero1α forms mixed disulfides with FAD (Flavin-Adenine-Dinucleotide) in order to promote disulfide bond formation. FAD, in this case, serves as an electron acceptor and will shuttle the donated electrons from Ero1α to molecular O_2 (Figure 1.3). The molecule Flavin-adenine-dinucleotide comes in two forms, FAD (oxidized) and $FADH_2$ (reduced) which is synthesized from the vitamin riboflavin and originates from the Citric Acid Cycle (or Krebs cycle) in mitochondria (Devlin 2002). FAD can exit the mitochondria and is then able to enter the cytosol. Furthermore, yeast Ero1p shows sensitivity towards these free FAD levels within the cytosol; this was discovered as *in vitro* experiments showed that a minor variation in physiologic FAD concentrations had substantial effects on Ero1p's activity (Tu and Weissman 2002). This could suggest a possible mechanism as to how the cell regulates oxidative protein folding. Moreover, this could also indicate that free FAD levels within the ER are regulated by a FAD-specific transporter (Tu and Weissman 2004). Such a transporter has indeed been discovered in yeast. Protchenko *et al* have demonstrated that so called FLC proteins are responsible for shuttling FAD into the ER lumen in yeast. These FLC proteins were initially thought to regulate heme uptake to stimulate growth in yeast (Protchenko *et al.* 2006).

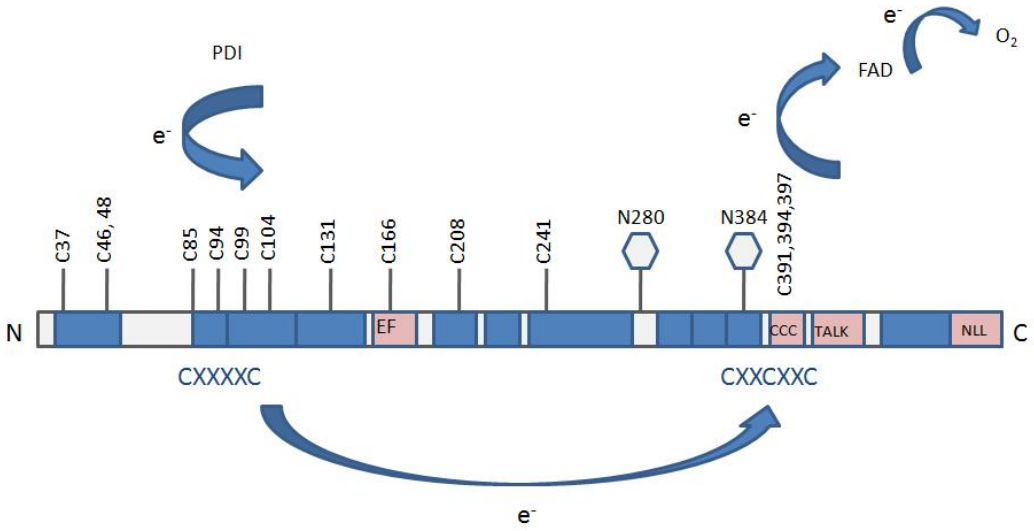

Figure 1.3: Ero1α and disulfide exchange. The schematic shows the structural and functional domains of Ero1α. All 'C's represent cysteine residues with their respective amino acid position. CxxxxC and CxxCxxC are the redox-active sites where PDI and FAD bind respectivaly. Blue arrows indicate the electron flow. (Modified from Dias-Gunasekara and Benkam, Biochemical Societt Transactions, 2005, Vol. 33).

Nevertheless, it is still not known, as to how FAD is being shuttled from the mitochondria and/or the cytosol into the endoplasmic reticulum, in eukaryotes.

The ER-resident protein ERp44 is induced by the unfolded protein response (UPR) (Anelli *et al.* 2002) and has been identified as a central sensor of the environmental state of the ER by regulating total Ca^{2+} concentrations via the IP3receptor type I (IP_3R1). This regulation lies within the direct interaction of ERp44 and with the third luminal loop of the IP3 receptor (Higo *et al.* 2005). ERp44 is also capable to interact with Ero1α at its cysteine residues C166 and C208 (Figure 1.3) by forming mixed disulfides. This interaction is thought to retain Ero1α in the ER (Anelli *et al.* 2003). Additionally, it has recently been discovered that Ero1α plays a significant role in the induction of apoptosis. It was demonstrated that CHOP causes the induction of Ero1α, which subsequently triggers release of Ca^{2+} via the IP3R (Li *et al.* 2009).

1.2 ER chaperones

It is essential for the cell to keep ER oxidative protein folding ongoing, because its block causes the accumulation of unfolded proteins within the ER that tend to aggregate and cause oxidative stress (Shen *et al.* 2004). Hence, ER chaperones are crucial as they mediate protein folding. Nevertheless, they are responsible for not only proper folding but also in determining which proteins are

correctly folded and hence can leave the ER or are misfolded in which case they need to be targeted for degradation (Buck *et al.* 2007).

The chaperone BiP (Grp78/Hsp70):

Proteins of the Hsp70 family (Heat-shock-protein-70) are found in many cellular locations. For instance in the nucleus, mitochondria, cytosol and in the ER where they are crucial for helping the protein folding process of newly synthesized proteins (Christis *et al.* 2008). Hsp70s are able to protect the hydrophobic sequences of not yet fully folded proteins which keeps them from aggregating (Christis *et al.* 2008). The chaperone BiP (Grp78) is a member of the Hsp70-family and resides within the ER lumen. Of all the Hsp70 family members, BiP is the most abundant (Guth *et al.* 2004). Its N-terminus contains an ATPase domain whereas the C-terminus is essential for peptide-binding (Christis *et al.* 2008). BiP is an important ER protein as it has a number of different functions. The chaperoning functions of BiP are required as newly synthesized polypeptide chains enter the ER lumen through the translocon. Because these polypeptide chains are not folded yet, they require the binding of BiP to their hydrophobic segments to prevent aggregation. Additionally, BiP binds to calcium as do other calcium-binding proteins within the ER, to regulate ER-calcium-homeostasis. Furthermore, BiP is capable of regulating the unfolded protein response (UPR) that is essentially triggered by ER-stress. In order to do so, BiP is bound to three ER-stress sensors that are located within the ER-membrane. ER-stress causes the

dissociation of BiP with these stress sensors, subsequently resulting in the activation of the unfolded protein response (see chapter 1.4 The Unfolded Protein Response) (Figure 1.4) (Figure 1.6) (Ni and Lee 2007).

The chaperones, calnexin and calreticulin:

Calnexin (CNX) and calreticulin (CRT) are lectin-like chaperones. This means that they are capable of recognizing and subsequently binding to the oligosaccharyl-appended N-glycan of a glycoprotein (Helenius and Aebi 2004). Calreticulin is found in the ER lumen. It is able to act as a chaperone but also to bind Ca^{2+}. Its N-terminal signal sequence facilitates translocalization into the ER after synthesis, while its C-terminal KDEL sequence facilitates retention to the ER (Michalak *et al.* 2009). This retention mechanism is controlled by the Golgi-membrane-bound KDEL receptor which is capable of retrieving ER soluble proteins back into the ER if they have escaped through the secretory pathway (Pelham 1990). Calnexin on the other hand is much larger in size than calreticulin and contains a transmembrane domain (Williams 2006). Both calreticulin and calnexin have been shown to be proficient in binding ATP, Ca^{2+}, and Zn^{+} and additionally they can bind to the thiol-oxidoreductase ERp57 (Baksh *et al.* 1995; Oliver *et al.* 1997; Corbett *et al.* 2000). The binding to ATP, Ca^{2+}, and Zn^{+} is essential for several reasons. First of all, calcium signaling as well as calcium homeostasis within the ER is regulated by proteins that are proficient in binding calcium. The influx of Ca^{2+} into the ER is mediated by Ca^{2+}-ATPases. The

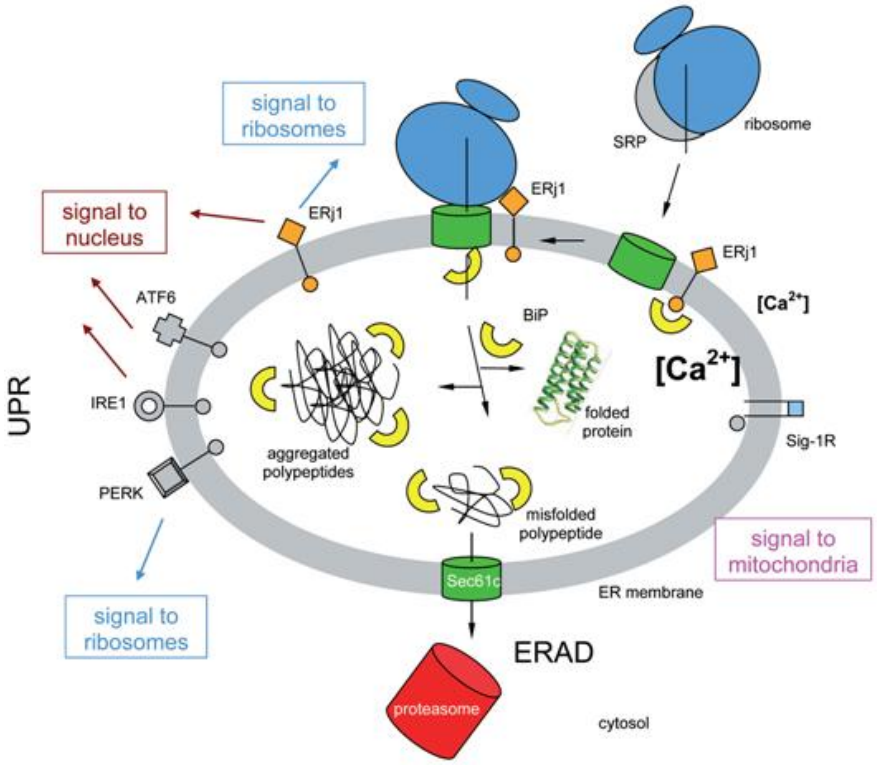

Figure 1.4: The relation of intra-ER processes. This schematic shows crucial events within the ER such as the activation of the UPR by aggregation of misfolded proteins and the ER-associated degradation. PERK, IRE1 and ATF6 are ER-stress sensors located in the ER membrane. The dissociation of BiP (shown in yellow) from these three ER-stress sensors will cause the upregulation of several genes to counteract aggregation of polypeptides within the ER. ERj1 is a transmembrane protein that is ususally found in close proximity to the translocon (shown in green). It ensures a stable interaction of the ribosomal complex (shown in blue) to the translocon. The ER-facing domain of ERj1 binds to BiP. This interaction ensures that BiP is found in close proximity to the newly synthesized polypeptide chains as they enter the ER lumen. SRP is the signal-sequence recognition particle that binds to the ribosome and leads it to the translocon where SRP binds to its receptor. BiP is also capable to bind to the sigma-1-receptor (Sig-1R) found in the ER membrane. Their dissociation results in sig-1R to bind to the IP3R which will subsequently cause the release of calcium into the cytosol. Misfolded proteins accumulate within the ER while BiP is still bound to them. These misfolded proteins are tagged for ERAD (ER-associated-degradation) which leads to their degradation in the proteasome (shown in red), in the cytosol. (Adapted from Dudek *et al*, 2009)

binding of Zn^+ to proteins that are involved in protein folding was shown to be linked to the thermodynamic properties of protein folding itself (Berg 1990). The binding to a metal ion such as Zn^+ allows for cross-linkage within the sequence of the protein thus resulting in more conformational stability of the protein (Berg 1990).

The chaperones calnexin and calreticulin are oligosaccharide-binding proteins that bind to the sugar-moieties of a newly synthesized glycoprotein. The addition of the oligosaccharide $Glc_3Man_9GlcNAc_2$ to the asparagine residue of the unfolded protein begins the process of *N*-glycosylation (Khalkhall and Marshall 1975). As seen in Figure 1.5, the glucose moieties at the A-branch are subsequently trimmed by glucosidase I and II. In the next step, UDP-glucose-glycoprotein glucosyltransferase (UGGT) acts as a quality control checkpoint and adds back a glucose residue (Taylor *et al.* 2004). The protein is now monoglucosylated ($Glc_1Man_9GlcNAc_2$) which is the recognition motif for the lectins calnexin or calreticulin (Parodi 2000). The removal of the last glucose-moiety by glucosidase II leads the glycoprotein into another round of quality control: the protein detaches from the CNX/CRT-complex and allows for UGGT for an additional assessment (Anelli and Sitia 2008). Figure 1.5 shows that all the Glc units are added to the mannose. In the first cycle when the glucose moieties are removed, mannose will not be removed by mannosidases at the same time to ensure faster re-glycosylation in case of misfolding (Trombetta and Parodi 2003). The trimming of mannose is a crucial step in quality control as it will prevent the addition of glucose to the protein which will subsequently lead the protein out of

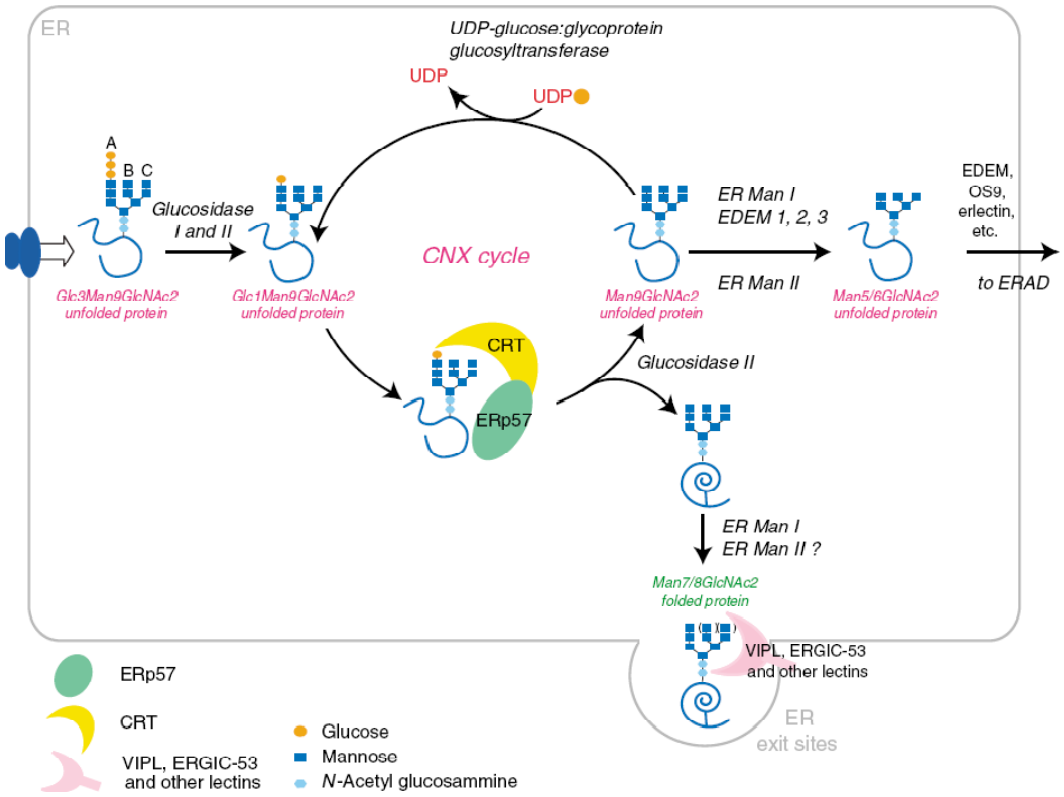

Figure 1.5: The calnexin/calreticulin cycle. This schematic shows glycosylation with the chaperones calnexin (CNX) and calreticulum (CRT) of glycoproteins that go into the CNX/CRT cycle and are then further processed. Shortly after the carbohydrade groups are added to the polypeptide chain, glucosidase I and II will remove the glucose moieties extept for one (shown in orange). CNX and CRT together with ERp57 can then bind to this polypeptide and lead it through the CNX/CRT-cycle. The re-addtion of a glucose unit is performed by UGGT (UDP-glucose:glycoprotein glucosyltransferase. Upon the completion of a fully folded protein, all glucose residues are removed. Mannosidase can lead to the trimming of the most upper mannose residues. This is a signal that is recognized by proteins such as EDEM (ER-degradation-enhancer-mannosidase-like) that will result in the degradation of this polypeptide. Proteins that have been folded properly leave the ER via ER exit sites. (Adapted from Anelli & Sitia, Embo 2006)

the CNX/CRT-cycle (Anelli and Sitia 2008). The new $Man_7GlcNAc_2$ folded protein is then ready for export via ER exit sites towards the Golgi network where it can then be distributed to its final destination.

The binding of either calreticulin or calnexin to a glycoprotein within the ER has two beneficial aspects for the not yet fully folded protein: it ensures retention to the ER and also guarantees that no further protein aggregation is possible which in turn allows for other oxidoreductases such as ERp57 to aid in the proper folding of the protein (Parodi 2000).

As mentioned earlier, calreticulin and calnexin are ER-resident proteins but have been shown to localize to a specific subdomain of the ER, the MAM (mitochondria-associated-membrane) (Hayashi and Su 2007). Interestingly, approximately 80% of calnexin is found on the MAM, indicating its significance in ER-mitochondria calcium channelling (Myhill *et al.* 2008). Chapter 1.5 will give further insight into the function of the MAM as well as focus on some of the proteins that are found there.

1.3 Quality Control

ER-quality control is the sum of the ER mechanisms that assure that only fully functional and fully folded secretory proteins are secreted from the ER. If quality control fails, proteins that are not able to obtain their native structure and are not tagged for degradation could essentially trigger a number of diseases. For

this reason, there are a couple of different mechanisms where ER quality control acts to prevent this from happening: a) proteins that are misfolded are being kept in the ER and chaperones aid in the rearrangement of their disulfide bonds; b) a permanent aggregation of misfolded proteins in the ER will lead to the translocation to the cytosol for proteasomal degradation (ERAD); c) some proteins are not folded completely but yet are able to reach the Golgi. In this case, quality control makes sure that these proteins are retained within the Golgi, are translocated back to the ER or will be sidetracked to lysosomes for degradation (Trombetta and Parodi 2003). Misfolding of proteins has been shown to be associated with a number of several diseases. As for neurodegenerative diseases, both Parkinson and Alzheimer patients show alleviated levels of misfolded proteins (post mortem) (Muchowski and Wacker 2005). Many patients that suffer from cystic fibrosis show a ΔF508 mutation which is located in the cystic fibrosis transmembrane regulator (CFTR). This mutation causes a number of defects including the misfolding of proteins (Powell and Zeitlin 2002).

ER-associated degradation (ERAD):

The terminal removal of all the glucose moieties and the trimming of mannose by ERManI result in the release of the protein from the CNX/CRT cycle. In some cases, proteins can have all their glucose moieties removed after having completed the CNX/CRT cycle, but are still not properly folded. These proteins

will then be recognized by specific lectins such as EDEMs and can be targeted for ER-associated degradation (ERAD) (Anelli and Sitia 2008).

But how can the ER differentiate between trimmed and misfolded proteins and properly folded proteins? Experiments have shown that the ER is indeed capable of differentiating these two scenarios from each other, simply by the length of time that the particular glycoprotein stays in the ER (Helenius and Aebi 2004). This time frame is estimated to be around 30 to 90 min followed by a decay and is regulated by EDEM which is a lectin that is able to bind to Man8 residues (Mancini *et al.* 2003; Molinari *et al.* 2003). As mentioned earlier, the trimming of mannose by ERManI brings the CNX/CRT cycle to a halt. A fully folded glycoprotein will now leave the ER whereas a misfolded one is "flagged" for degradation. Clearly, ERManI cannot be the only factor to target a protein for degradation. Seemingly, ERManI must be proficient to team up with members of the EDEM (ER-degradation enhancing alpha mannosidases like protein) family to efficiently target glycoproteins for degradation (Hirsch *et al.* 2009). In the following steps, ubiquitin ligases that are located cytoplasmic face of the ER (Ramadan *et al.* 2007), recognize the misfolded proteins and will subsequently flag them by ubiquitination (Hirsch *et al.* 2009). These tagged misfolded proteins are then shuttled toward the 26S proteasome in the cytosol, which is thought to be accomplished by the Cdc48/p97 complex (ATPase) (Nakatsukasa and Brodsky 2008).

1.4 The Unfolded Protein Response (UPR)

The unfolded protein response (UPR) is a signaling mechanism to avoid ER stress. ER stress is an imbalance that arises when ER function and ER capacity can no longer meet its demands resulting in the accumulation of misfolded proteins (Ni and Lee 2007). Under normal conditions, processes such as post-translational modifications, oxidative protein folding and quality control, just to mention a few, are regulated with the help of ER chaperones (Ni and Lee 2007). Generally speaking, the unfolded protein response (UPR) is a signaling cascade to ensure the survival of the cell. The UPR will allow for the activation of three main branches that are all initiated by three transmembrane proteins: IRE1 (inositol requiring enzyme 1), PERK (ER resident transmembrane kinase) and ATF6 (activating transcription factor 6) (Schröder and Kaufman 2005; Davenport 2008; Ron and Hubbard 2008). When inactive, all of these three proteins are in a bound state with the chaperone BiP (Grp78). ER stress in turn, causes the disassociation of these transmembrane proteins from the chaperone BiP (Figure 1.6) (Davenport 2008). Protein synthesis comes to a halt and the upregulation of certain genes come into effect (Ron and Hubbard 2008). This activation of certain transcriptional programmes will then take control in making the final decision between cell death and survival (So *et al.* 2009). If the UPR is incapable to reinstate ER homeostasis by clearing the amount of unfolded proteins, it is inevitable for the cell to activate apoptotic -inducing mechanisms such as the upregulation of CHOP and caspases (Lai *et al.* 2007).

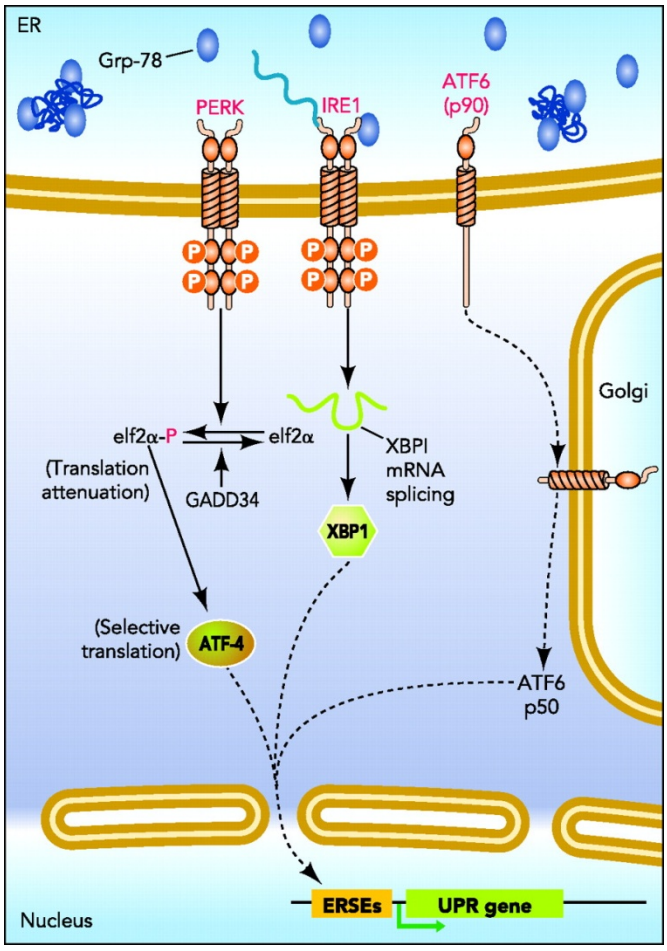

Figure 1.6: The unfolded protein response and its sensors. Upon ER stress, the stress sensors IRE1, PERK and ATF6 dissociate from the chaperone BiP. PERK that is no longer bound to BiP will phosphorylate itself to dimerize, followed by the phosphorylation of the eukaryotic translation initiation factor 2α (eIF2 α). The dissociation of BiP and IRE1 will also allow for IRE1 to dimerize. Subsequently, the activated form of IRE1 will cause the unconventional splicing of mRNA of X-box-protein1 (Xbp1) due to its endonuclease activity. ATF6 will undergo protelolysis and result in a ATF6p50 fragment. All of these translocate to the nucleus where they bind to ER-stress elements (ERSE) which will instigate the upregulation of genes required to counteract ER stress. (Adapted from Lai, E. *et al*. Physiology, 2007)

The role of the three ER-stress-sensors IRE1, PERK and ATF6:

IRE1 was the first stress-receptor to be discovered. Interestingly, this kinase is only known to phosphorylate itself as no other targets have yet been identified (Ron and Hubbard 2008). Upon stress, IRE1 dimerizes and will then autophosphorylates itself which in turn causes the unconventional splicing of Xbp1(X-box binding protein1) mRNA due to its endonuclease activity (Bernales *et al.* 2006). The nonconventional splicing of Xbp1 results in its activation and its transcription activator will then drive the expression of genes to increase the amount of ER chaperones (Lin *et al.* 2007).

Another interesting aspect of IRE1, besides its role in cell survival, is that it is also considered to be part of triggering cell death under long-term ER-stress conditions (Kim *et al.* 2006; Lin *et al.* 2009). Attenuated ER-stress levels cause IRE1 to switch from the non-conventional splicing of Xbp-1 to activating JNK signaling pathways as well as selectively interacting with the BCL-2 family members such as Bak and Bax (Urano *et al.* 2000; Hetz *et al.* 2006). Activated Bak and Bax can translocate to the outer mitochondrial membrane where they oligomerize. Eventually, these two proteins cause the outer mitochondrial membrane to permeabilize which results in the release of cytochrome c, triggering a caspase cascade to initiate apoptosis (Wong and Puthalakath 2008).

The transmembrane protein PERK is usually bound to the ER chaperone BiP under resting conditions. The accumulation of unfolded proteins within the ER causes also the disassociation with BiP, as is the case with IRE1 (Davenport

2008). Upon disassociation with BiP, PERK dimerizes and autophosphorylates itself which results in its activation (Lai *et al.* 2007). Activated PERK is then able to phosphorylate serine-51 on eIF2α (eukaryotic initiation factor 2α) (Lai *et al.* 2007). The phosphorylation of eIF2α essentially brings a halt to global protein synthesis (Prostko *et al.* 1993) but at the same time initiates the translation of ATF4 (Activating transcription factor 4) mRNA (Lai *et al.* 2007). The expression of genes that are involved in oxidative stress, amino acid synthesis, angiogenesis etc, rely on the regulation by ATF4 (Ameri and Harris 2008).

ATF6 (Activating transcription factor 6) is the third ER-stress sensor and also an ER transmembrane protein. Unlike IRE1 and PERK, it is not a kinase but rather a transcription factor as the name implies. ATF6 is a bZIP (basic leucine zipper) protein that, when activated, will bind to ER-stress response element (ERSE) -containing genes such as *grp* (glucose-regulated-protein) genes to induce their promoter (Yoshida *et al.* 1998; Li *et al.* 2000). ER stress causes ATF6 to generate, by means of proteolysis, a new fragment called ATF6(p50) which translocates to the nucleus to activate transcription (Shen *et al.* 2004). This proteolyic process takes place at the Golgi and is also known as regulated intramembrane proteolysis (RIP) (Sommer and Jarosch 2002; Benjamin 2006).

1.5 Signaling to mitochondria at the MAM

The mitochondria-associated-membrane (MAM) is thought be a physical bridge that connects the ER with mitochondria. The idea of the existence of such a membrane domain was established in the 1960's, but the evidence for its existence was only shown years later in 1990 by several research groups (Hayashi *et al.* 2009). It is estimated that less than 12% of the outer mitochondria membrane form the MAM (Csordas *et al.* 2006). One of the first processes to be identified to occur at the MAM was the non-vesicular transport of phospholipids. It was the general understanding that phospholipid biosynthesis takes place on ER membranes, with the exception of some enzymes that would be constrained to mitochondria (van Meer 1989). The examination of phospholipid biosynthesis throughout the cell led to the conclusion that only 5% of this synthesis was done by the Golgi (Vance and Vance 1988). This discovery, however, meant that there is a different mechanism other than vesicle-mediated transfer to move phospholipids between membranes (Achleitner *et al.* 1999; Levine and Loewen 2006). It was hypothesised that subdomains of the ER exist which are linked to the mitochondria. Interestingly, research done by other groups had shown by electron microscopy that mitochondria were indeed tethered to the endoplasmic reticulum by some sort of 'strands' (Baranska 1980). Electron microscopy data have shown that the linkage of the ER with mitochondria is established by tethers which contain both smooth and rough ER and are in contact with mitochondria resulting in the formation of the MAM (Csordas *et al.* 2006). The functioning of

the MAM in mammalian cells has been described by several proteins that were found there, including mitofusin-2 and grp75. Mitofusin-2 is a GTPase that has been shown to form interorganellar bridges between the ER and its subdomain, the MAM (de Brito and Scorrano 2009). Cytosolic grp75, on the other hand, has been found to connect IP3receptors to VDAC1 (Voltage-dependent anion channel 1) (Szabadkai *et al.* 2006), thus forming these so called tethers.

Figure 1.7 and Figure 1.8 both demonstrate some of the protein-protein interactions that take place at the MAM. As seen in Figure 1.7, the MAM is enriched with proteins that are involved in calcium-channelling. For instance, we find the Ca^{2+}-ATPase at the MAM with calnexin and calreticulin bound to it. This leads to the influx of calcium into the ER lumen. Furthermore, we find IP3 receptors of the type 3 (IP3R3) at the MAM. These are activated by the binding with the sigma-1 receptor. BiP regulates this activity by associating with the sigma-1 receptor which in turn cannot bind to IP3R3. Only the release of BiP from the sigma-1 receptor can result in the association with IP3R3 thus causing the release of calcium into the ER lumen.

1.6 Hypoxia and hypoxic tumors

Hypoxia is the decrease of oxygen within the body and within cells. Hypoxic stress can either lead to cell death by inducing apoptosis or necrosis, or it

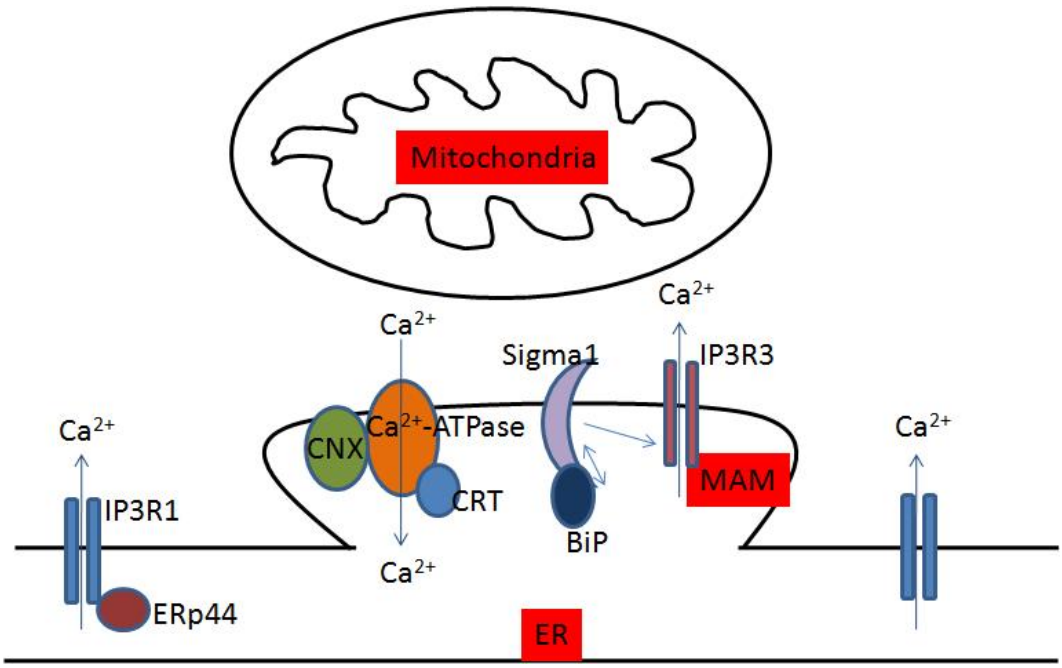

Figure 1.7: Protein-receptor interactions at the MAM. Chaperones regulate mitochondrial and ER Ca^{2+} signaling. ERp44 binds to the type-1 IP3R; which causes a block of calcium release; CNX and CRT both interact with the Ca^{2+}-ATPase to allow for Ca^{2+} influx into the ER lumen; BiP/GRP78 binds to the inactive form of the Sigma-1 receptor. The dissociation of BiP causes Sigma-1R to bind to the IP3R3 which activates Ca^{2+} release from the ER into the cytosol. (Modified from T. Hayashi *et al.*, Trends in Cell Biology, 2009)

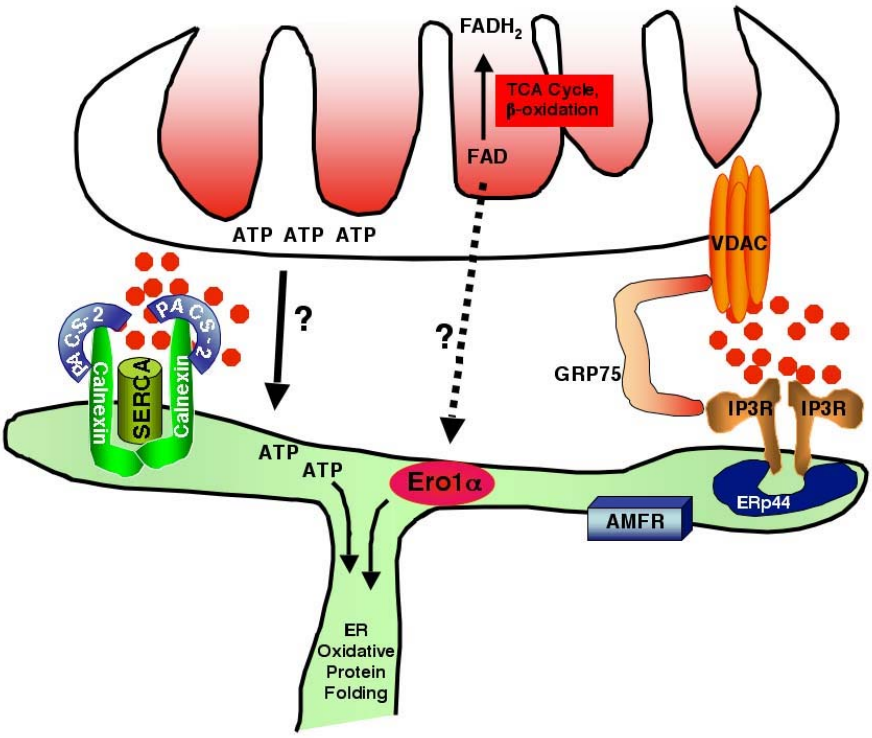

Figure 1.8: Overview of selected proteins found on the MAM. Metabolism within the mitochondria and production of ATP both influence ER oxidative protein folding. This diagram shows some of the protein-protein interactions that have been found on the MAM. SERCA (sarcoplasmic/endoplasmic Ca^{2+}-ATPase) is required for Ca^{2+} influx into the ER. The chaperone calnexin can regulate SERCA by binding to it. This interaction is fascilitated by PACS-2, a multifunctional sorting protein within the cytosol. Energy in form of ATP is required for several processes within the ER. It is therefore nessesary that ATP, which is produced in mitochondria, is transported into the ER. It is unknown how ATP is inserted into the ER. The ER luminal protein Ero1α is also found on the MAM. This could be due to the fact that it requires FAD from mitochondria to function properly. Is remains unknown how FAD is shuttled into the ER in mammalian cells. The autocrine motility factor receptor (AMFR) has been found at the transitional ER. It has ubiquitin ligase activity and is an ER transmembrane protein. The IP3 receptor fascilitates the Ca^{2+} efflux out of the ER which is mediated by the interaction with the ER soluble protein ERp44. The voltage-dependent-anion-channel (VDAC) is located in the outer mitochondrial membrane and is responsible for Ca^{2+} uptake into mitochondria. VDAC and IP3R are in close proximity. The cytosolic chaperone Grp75 facilitates the interaction of both VDAC and IP3R to allow for Ca^{2+} signaling between the ER and mitochondria.

can lead to an adaptive response that will increase glycolysis and angiogenesis (Lee *et al.* 2007). Additionally, most tumors tend to be hypoxic due to the limited blood flow and oxygen circulation.

The three top factors that trigger tumorigenesis are abnormal cell-cycle regulations, unusual overexpression of oncogenes and mutations of tumor-suppressor-genes (Brahimi-Horn *et al.* 2007). Conversely, it has been well established that other factors contribute to tumorigenesis, in particular hypoxia (Brahimi-Horn *et al.* 2007). The correlations of hypoxic, metastasizing tumors with poor prognosis in terms of patient survival rates make it a necessity to further investigate the role of hypoxia.

It is important to note that not all cancer cells increase the amount of glycolysis in the same way but rather show different mechanisms, which is probably due to their mutation patterns that can vary in each tumor (Moreno-Sánchez *et al.* 2009). One of the goals in cancer research is to conduct a wide-ranged analysis of different patterns of glycolytic pathways. This would allow for better predictions regarding glycolysis rates in tumors (Moreno-Sánchez *et al.* 2009). What has become clear is the fact that metastasizing tumors show elevated levels of HIF1α expression and glycolytic enzymes which lead to high rates of glycolysis whereas non-metastasizing tumors lack all of these unless they are exposed to hypoxia (Moreno-Sánchez *et al.* 2009). Not only do metastasizing tumors show resistance to chemo- and radiotherapy due to their mutations but also

show an increase in lymphatic spread and the very high likelihood of reoccurrence (Hockel *et al.* 1996).

1.6.1 Hypoxia-inducible-factor (HIF)

The Hypoxia-Inducible-Factors (HIFs) are a group of transcription factors that are partially responsible for deciding which of the two fates the cell will undergo: apoptosis or survival, by triggering adaptive responses (Brahimi-Horn and Pouyssegur 2006; Lee *et al.* 2007). HIF1 is a heterodimer that consists of two subunits, α and β (Fandrey and Gassmann 2009). Under normoxia, HIF1α is bound to a prolyl hydroxylase enzyme (PH) through hydroxylation of a proline residue in the HIF1α domain. Once this complex is formed, pVHL can then bind to HIF1α and cause its degradation by the proteasome by means of ubiquitination (Maxwell *et al.* 1999; Zhu and Bunn 2001). If the cells are experiencing hypoxic stress, proline can no longer be hydroxylated and thus not be degraded. This allows for HIF1β, which is found in the cytosol, to bind to HIF1α and form a heterodimer which will then translocate to the nucleus via importins which are nuclear transport receptors (Depping *et al.* 2008). Once in the nucleus, the HIF1α/β-heterodimer binds to the Hypoxia-Response-Element (HRE) and activates genes such as VEGF (angiogenesis), EPO (erythropoiesis), i-NOS and HO-1 (vasolidation) (Semenza 2000), but also upregulates the expression of Ero1α (Gess *et al.* 2003). The consequences of these upregulations lead ultimately to metastasizing tumors.

Interestingly, Ero1α is under the control of HIF1α. A better understanding of Ero1α and its correlation with hypoxia would be considered necessary if we want to fully explore all functions of Ero1α. This could then lead to the enhanced comprehension of hypoxic tumors.

1.6.2 The Warburg Effect

In the beginning of this chapter, hypoxia was characterized as the decrease of oxygen within the tissue and cells. In spite of this, cancerous cells have the ability to switch metabolic pathways even in the presence of certain nutrients. The first person to further characterize this was Otto Warburg. He hypothesized in the early 20th century that cancer is a 'mitochondrial dysfunction' because cells no longer generate ATP through ways of a breakdown of pyruvate and consuming oxygen, but through means of glycolysis (Denko 2008). Under normal conditions, all cells generate energy (ATP) by mitochondrial oxidative phosphorylation. This metabolic pathway involves the oxidation of nutrients which are chemically processed into free energy (ATP). Cancer cells, however, switch from oxidative phosphorylation to aerobic glycosylation which means that they consume glucose and turn it into lactic acid (Figure 1.9) (Yeluri *et al.* 2009). This is a very inefficient way of producing ATP but yet cancer cells persist to retain this process.

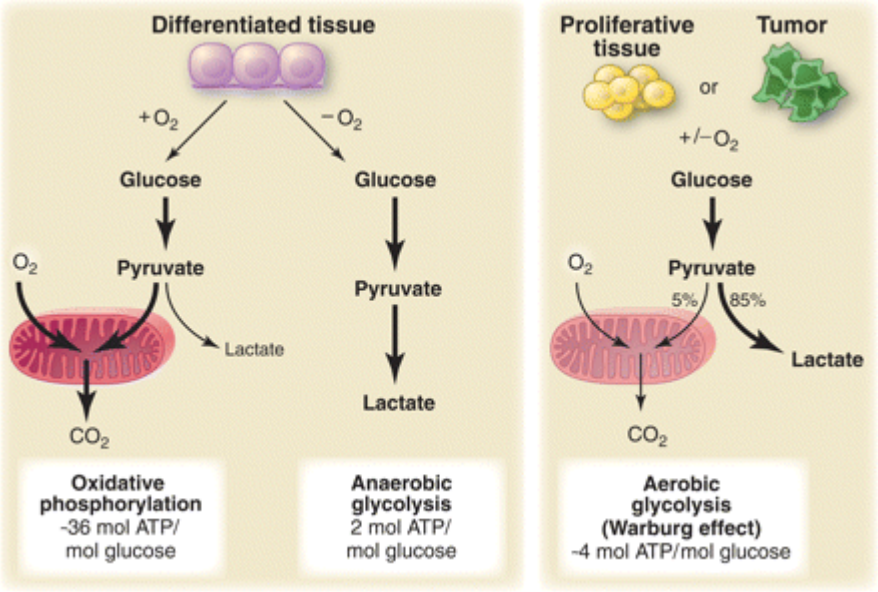

Figure 1.9: The Warburg-effect. In this schematic, it is shown how the cells can produce energy (ATP) by using glucose via oxidative phosphorylation or by anaerobic glycolysis. Hypoxic tumors tend to produce ATP by aerobic glycolysis regardless of oxygen amounts and will eventually produce lactic acid. (Adapted from Matthew G. Vander Heiden, *et al*; 2009)

Chapter 2 – Materials and Methods

2.1 Materials

All chemicals were used according to the manufacturer's specifications as well as in accordance with the protocols set out by the Environmental Health and Safety of the University of Alberta and Workplace Hazardous Materials Information System (WHMIS).

2.1.1 Chemicals, Reagents and other Materials

Acetone	EMD
Acrylamide/Bis	BioRad
Agar	BD
Agarose	Invitrogen
Antimycin	Alexis Biochemicals
Ammonium persulfate (APS)	BioRad
Ampicillin	Sigma
β-mercaptoethanol	BioShop
Bromophenol blue	Bio Rad
Complete 25x protease inhibitor	Roche
Cycloheximide	Sigma
DTT	Fisher Scientific
Dulbecco's modified eagle medium (DMEM)	Gibco
Ethanol	Commercial Alcohols
EDTA	EMD

EGTA	Sigma
Fetal bovine serum (FBS)	Gibco
Glycerol	Anachemia
HEPES	Sigma
Hydrochloric acid	Fisher Scientific
Kanamycin	Sigma
Licor blocking solution	LI-COR Biosciences
Methanol	Fisher Scientific
NEM	Sigma
Trans-Blot Nitrocellulose	Bio Rad
Oligomycin	Fermentas
Opti-MEM	Gibco
Optiprep	Sigma
PBS	Sigma
Rotenone	Sigma
Saponin	Fluka
Sodium azide	ICN Biomedicals Inc.
Sodium dodecyl sulphate (SDS)	J.T. Baker
Sucrose	EMD
Trichloroacetic acid (TCA)	Sigma
Tetramethylethylenediamine (TEMED)	OmniPur/EMD
Thapsigargin	Alexis Biochemicals
Tris	Bio Basic Inc.
Trypsin	Gibco
Tunicamycin	Alexis Biochemicals

Ultra centrifuge tubes	Beckman
Whatman Chromatography Paper	Fisher Scientific

2.1.2 Antibodies

Primary Antibodies:

The mouse monoclonal anti-Ero1α and the polyclonal anti-ERp44 were a kind gift from Dr. Roberto Sitia, Milan, Italy. The antibodies mouse anti-myc and GAPDH were provided by Dr. Tom Hobman, Edmonton, AB. The rat anti-AMFR antibody was a kind gift from Dr. Robert Nabi.

▪ Rabbit anti-Calnexin (our lab)	Open Biosystems, Huntsville, AL/
▪ Mouse anti-ComplexII	Mitosciences, Eugene, OR
▪ Mouse anti-Mitofusin-1	Abnova, Taipeh, Taiwan
▪ Rabbit anti-Mitofusin-2	Sigma, Oakville, ON
▪ Mouse anti-PDI	ABR, Golden, CO
▪ Mouse anti-BiP (Grp78)	BD, Franklin Lakes, NJ
▪ Rabbit anti-Calreticulin	ABR, Golden, CO
▪ Rabbit anti-Acat1	ABR, Golden, CO
▪ Rabbit anti-eIF2α	Cell Signaling, Boston, MA
▪ Mouse anti-βCOP	Genetex Inc., Irvine, CA
▪ Human anti-VEGF165	Humanzyme, Chicago, IL

Secondary Antibodies:

All secondary antibodies that were used during my project were AlexaFluor-conjugated (1:5,000) (Invitrogen):

- AlexaFluor680 goat anti-mouse IgG (H+L)
- AlexaFluor750 goat anti-rabbit IgG (H+L)
- AlexaFluor680 goat anti-rat IgG (H+L)

2.1.3 Buffers and other solutions

- Stacking Buffer (4x): 1.5 M Tris, pH 6.8 and 0.4 % SDS
- Separating Buffer (4x): 1.5 M Tris-HCl (pH 8.8) and 0.4 % SDS
- Homogenization Buffer: 250 mM sucrose, 10 mM HEPES-NaOH (pH 7.4), 1 mM EDTA, 1 mM EGTA
- 5X SDS-Page Loading Buffer: 50 % (v/v) glycerol, 10 % SDS (w/v), 0.312 M Tris (pH 6.8), 0.2 % Bromophenol blue, 25 % (v/v) β-mercaptoethanol, and top up with H_2O.
- 10x SDS Running Buffer: (for 1 L: 30.25 g Tris, 144 g Glycine, 10 g SDS)
- CHAPS Buffer: 1 % CHAPS, 10 mM Tris/HCl pH 7.4, 150 mM NaCl, 1 mM EDTA
- RIPA Buffer: 50 mM Tris/HCl pH 7.5, 150 mM NaCl, 1 mM EGTA (pH 8), 1 mM EDTA (pH 8), 1 % TritonX100, 0.1% SDS, 0.1% NaDOX (sodium deoxycholate)

- 1x PBS: 137 mM NaCl, 2.7 mM KCl, 10 mM Na_2HPO_4, 1.76 mM KH_2PO_4, pH 7.4
- IF washing Buffer: (for 500 ml: 500 ml PBS^{++}, 2.5 ml 20 % TX-100, 1 g BSA)
- 20x Carbonate Transfer Buffer: (for 500 ml: 8.4 g $NaHCO_3$, 3.2 g Na_2CO_3)
- Transfer Buffer: 1x Carbonate Transfer Buffer + 20 % Methanol +H_2O
- TBS-T: 10 mM Tris-HCl (pH 8), 0.15 M NaCl, 0.05 % TritionX100, 0.01% NaN_3

2.1.4 Plasmids

Figure 2.1 lists all Ero1α mutants that were previously generated by Dr. Thomas Simmen.

2.2 Methods

2.2.1 Cell culture, Transfection and Lysis

The HEK293T and HeLa cells (obtained from ECACC UK) were cultured in DMEM (Invitrogen, Carlsbad, CA) containing 10 % fetal bovine serum (Invitrogen, Carlsbad, CA) and kept at 37°C in an incubator containing 95 % air and 5 % CO_2.

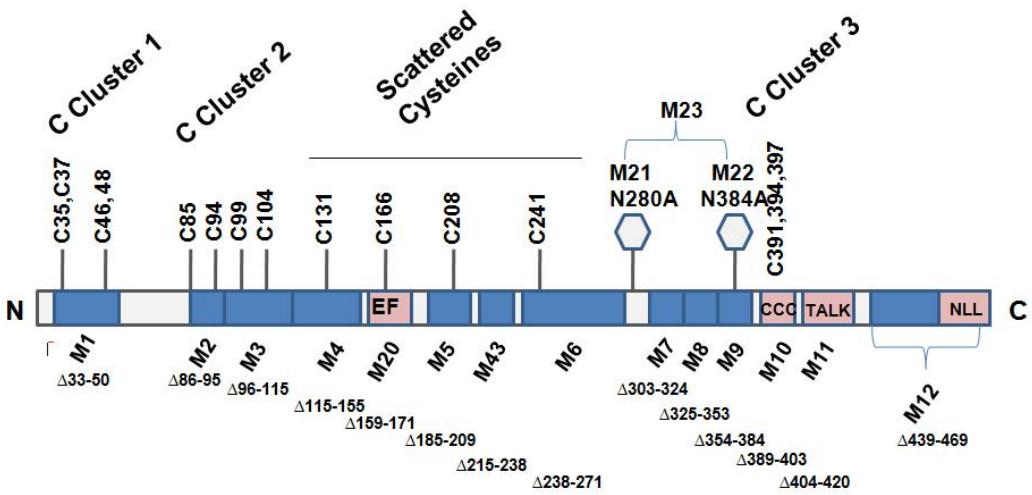

Figure 2.1: Ero1α mutants. The schematic lists all cysteine residues in wild type Ero1α and shows deletion mutants with blue boxes. All deletion mutants start with an 'M' with deleted residues as indicated. Hexagons indicate glycosylation sites. Cysteine residues are indicated by a 'C' followed by a number indicating its position within the amino acid sequence.

The human melanoma tissues were obtained from the Alberta Tumor Bank, Edmonton, AB.

Cells were seeded and transfected the following day. The cells were transfected using the transfection agent Metafectene Pro (Biontex, Germany) in accordance with the manufacturer's instructions/ transfection protocol.

Two days following transfection, the cells were prepared for lysis for further analysis. First, the cells were washed 3x with PBS^{++} (1x PBS, 0.5 mM $MgCl_2$, 1 mM $CaCl_2$) to ensure that no DMEM containing fetal bovine serum was still present as this would interfere with the later steps of the gradients and with the detection of proteins by Western blot. 500 µl of Chaps Buffer (containing complete protease inhibitor) were added to each 10 cm Petri dish. If the cells were transfected and had been grown in 6-well-plates, a total amount of 700 µl was used to obtain enough cell lysate for homogenization. After the cells had been harvested, all the lysates were collected and centrifuged at 4°C for 10 min at 800 g to pellet the nuclei and cell debris. The supernatant was then processed further according to the experiment (See section 2.2.6).

2.2.2 Human melanoma tissue

Tissue samples were cut into pieces weighing between 50 to 150 mg. The samples were kept at a frozen state with liquid nitrogen and were carefully ground with a pestle until they were powder-like. This powder was then transferred into a

2 ml microcentrifuge tube and 3x the volume of RIPA buffer, containing protease inhibitor, was added. The samples were then left on ice at 4◦C for 5 min to allow for the detergent in the buffer to take effect. The homogenization was performed using a T10 basic ULTRA-TURRAX from IKA. The samples were homogenized 3 times for approximately 30 s each, followed by a centrifugation step at 4◦C, for 10 min at 16.1 rcf. The resulting supernatant was transferred into a new microcentrifuge tube and the protein concentration was measured using a Pierce bicinchoninic acid (BCA) assay. The control tissue was from normal human skin and was obtained from Leinco Technologies.

2.2.3 VEGF secretion assay

Non-transfected HeLa cells were seeded at 7 x 10^5 to 9 x 10^5 cells/well and cultured in 6-well-plates. Transfected cells were seeded according to the transfection agent protocol. The cells were then incubated for 24 to 72 h in a hypoxic environment containing 1 % molecular oxygen. The supernatant was obtained and proteins were precipitated using the TCA precipitation assay (section 2.2.5). 30 µl of 2x sample buffer was then added to the protein pellets which were subsequently boiled for 7 min at 100°C, followed by analysis with SDS-PAGE.

2.2.4 Immunofluorescence

To visualize mitochondria, we used MitoTracker. A dilution of 1:1000 (in OptiMem) was required and had to be added to the cells 30 min prior to the start of the experiment.

A humid chamber (simple plastic box with moist paper towel) was prepared prior to starting the immunofluorescence. The cover slips that contained the cell on them were then washed 3 times in PBS^{++} in the six-well dish. After the fixing with 1 ml of 4 % paraformaldehyde in PBS^{++} in the six-well dish, the cells were incubated at room temperature for 20 min. This was followed by 3 washes with PBS^{++}. The cells were permeabilized for 1 min in IF wash buffer (see Buffer section) and blocked with 2 % BSA, 0.1 % saponin in PBS^{++}. The specific primary antibody (which should be diluted in 2% BSA and 0.1% saponin in PBS^{++}) was then added to the cover slips and was incubated for at least 1 h (on the parafilm were 30 µl of a 1:1000 dilution of the primary antibody). Note: it is important to turn the cover slips face down onto the drops while the incubation should take place in complete darkness to avoid bleaching of the antibodies. Following the incubation in the primary antibody, the cover slips were returned into the 6-well-plate with the right-side up and washed again 2 x with PBS^{++}. The old parafilm containing the primary antibody was to be removed from the humid chamber and a new one was prepared that contained drops of 30 µl of a 1:2000 dilution of the secondary antibody. The cover slips were placed onto the drops, face down, and incubated at room temperature for another 30 min in the dark.

Following this incubation, the cover slips were returned into the 6-well-plate, face up, washed again 2x with PBS^{++} and ultimately with dH_2O. The cover slips were then placed, face down, onto a drop of ProLong Antifade resin. The slides were then stored at 4°C in the dark.

2.2.5 TCA precipitation

For the TCA precipitation, an equal volume of 50 % TCA (trichloroacetic acid) was added to the protein sample so that the end concentration was 25 %. The samples were left on ice for 15 min which was followed by a centrifugation at 4°C for 15 min at 16.1 rcf. The supernatant was carefully aspirated and discarded. 300 µl of cold acetone (90 %) was then added to the remaining pellet in the microcentrifuge tube. This mixture was subsequently centrifuged for 5 min at 4°C at 16.1 rcf. The supernatant was removed and the pellet in the microcentrifuge tube was left to air dry for approximately 30 min. The samples were re-suspended in SDS-PAGE loading buffer (see buffers) and boiled for 5 min at 100°C. (Note: It is important to check for acidity of the sample by observing the color of the sample buffer. If it turns yellow, the addition of a few drops of 1 M Tris pH 8.8 is necessary to turn the sample blue again).

2.2.6 Optiprep gradients

For the optiprep gradient, I first prepared 25 %, 20 %, 15 %, 10 % and 5 % dilutions of optiprep (60 % iodixanol in water) in Homogenization Buffer (see Buffers). These dilutions were then layered (800 µl of each) with the highest percentage (25 %) at the bottom of the centrifugation tube and the lowest percentage (5 %) at the top of all the other layers. The gradient had to equilibrate vertically for approximately 3 h at room temperature. While the gradients were equilibrating, the cells were washed 3 times with PBS^{++}. After the washing on ice, 500 to 700 µl of a Homogenization buffer/Protease inhibitor mixture was added to the cells. With this buffer on, the cells were then scraped off the petri dish with a cell-scraper (BD). The harvested cells can then be passed through an 18 micron clearance-ball-bearing-homogenizer with a total of 25 passages. The resulting homogenates were collected in eppendorf tubes and centrifuged for 10 min at 800 g to pellet the nuclei and the cellular debris. The supernatant was then carefully layered on top of the optiprep gradient and centrifuged for 3 h at 32,700 rpm (Sw55Ti rotor). Following centrifugation, the supernatant was split into 6 fractions (each about 833 µl) and collected in microcentrifuge tubes. The proteins in each fraction were then precipitated by TCA precipitation (see protocol). The protein sample was re-suspended in 25 µl of sample buffer and 5 µl of 1 M Tris, pH 8.8 to reduce acidity of the samples. The samples were boiled for 5 min at 100°C and analyzed by SDS-PAGE, followed by a western blot.

2.2.7 Western blotting

The proteins on the SDS-PAGE were transferred to a nitrocellulose membrane (BioRad) by overnight transfer in a transfer-apparatus. The transfer was performed overnight using 15V at 4°C. Following a successful transfer, the membrane was blocked with LICOR blocking solution for 30 min at room temperature. The membrane was then incubated for 1 h or more in the primary antibody (diluted in milk) at 4°C on a shaker. Subsequent washing of the membrane two times for 5 min with 1x TBS-T (see Buffer section) was necessary to rid any unbound primary antibody. This wash was followed by the incubation of the membrane with the secondary antibody (also diluted in milk; 1:5,000) for 30 min on a shaker at room temperature. The membrane was again washed 3 times for 5 min with 1x TBS-T. The 1x TBS-T was discarded and some ddH_2O (double distilled) was added to the membrane to prevent drying out.

Chapter 3 – Results

3.1 Co-localization of Ero1α and mitochondria

The key players in disulfide bond formation required for oxidative protein folding are PDI (Protein Disulfide Isomerase), and Ero1 (ER-oxidoreductin 1). For their correct functioning, these two enzymes and others involved in oxidative protein folding require a steady input of metabolites from mitochondria, including oxidized FAD (Flavin-Adenine-Dinucleotide) (Tu and Weissman 2002) and ATP (Braakman *et al.* 1992). Furthermore, Ero1 also requires molecular oxygen. Together, these observations indicate that oxidative protein folding depends on the correct functioning of mitochondria and might therefore depend on the opposition of the ER to mitochondria. Thus, considering Ero1α's function in oxidative protein folding and its functional dependence on FAD, we wanted to determine if human Ero1α is enriched on a specific ER-subdomain.

We decided to investigate the localization of Ero1α to domains of the ER first by immunofluorescence. HeLa cells were cultured and prepared for immunofluorescence to examine the intracellular distribution of endogenous Ero1α. Figure 3.1 shows that the reticular pattern of Ero1α overlaps to some extent with mitochondria, indicating that Ero1α, a known ER protein, could localize to the vicinity of mitochondria and the mitochondria-associated-membrane (MAM). Additionally, a nuclear signal of Ero1α was also observed in Figure 3.1. This observation requires further tests if the nuclear staining pattern of Ero1α persists.

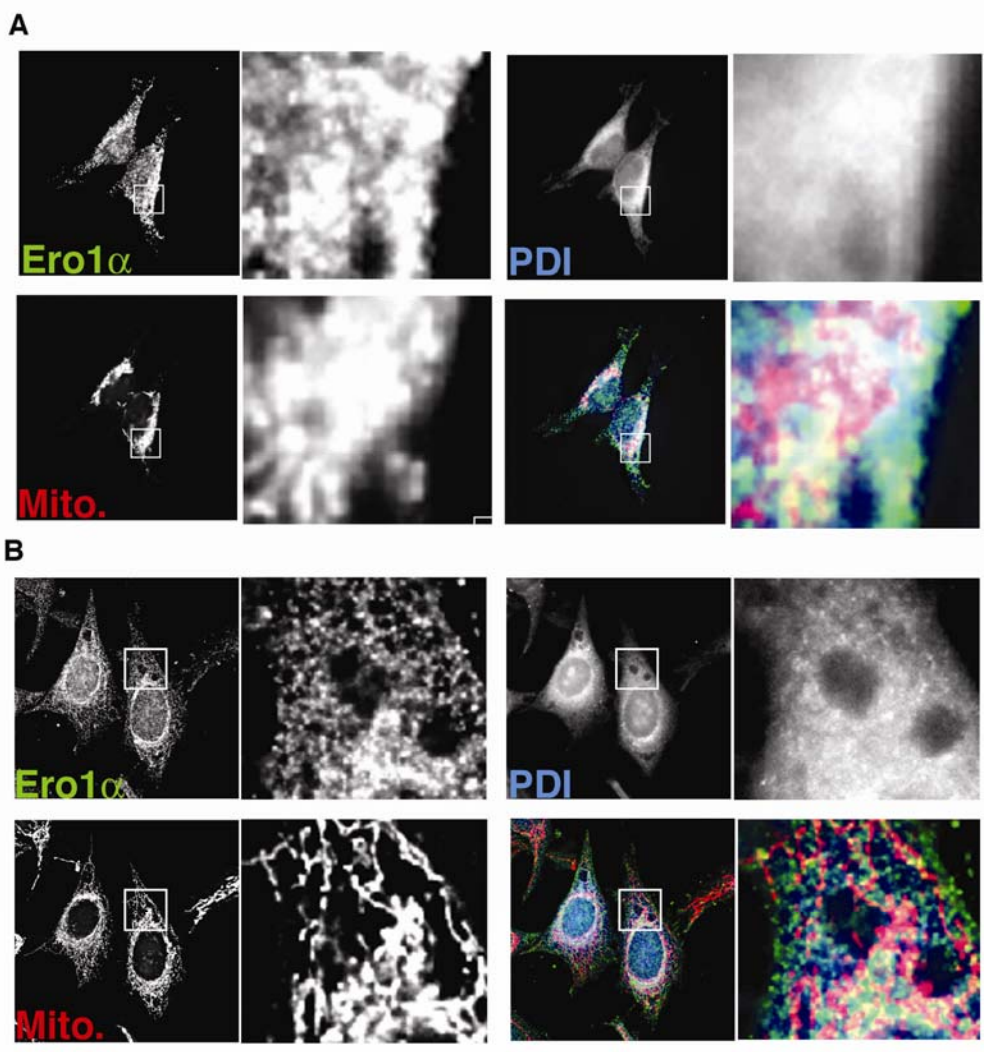

Figure 3.1: Ero1α co-localizes with mitochondria and ER. Co-localization of endogenous Ero1α with mitochondria (Mitotracker/red) and ER (indicated by the ER-resident protein PDI, blue) by immunofluorescence. Panel A shows the localization of Ero1α in HEK293T cells and Panel B in HeLa cells. Co-localization (white) of Ero1α (green), mitochondria (red) and ER (blue) is shown in the box.

3.2 Biochemical analysis of the localization of Ero1α

A partial co-localization of Ero1α with mitochondria and the endoplasmic reticulum was seen in Figure 3.1. This suggested the possibility of Ero1α to localize to the MAM, as observed with other ER proteins such as calnexin (Myhill *et al.* 2008). To test this possibility, we next attempted to biochemically separate the different subdomains of the ER. In order to isolate the MAM from the other domains of the ER, we decided to use optiprep gradients, because we had used this method successfully in the past (Myhill *et al.* 2008). This fractionation will fractionate membranes simply by the flow through a discontinuous or continuous gradient due to density. Thus, this will allow a separation of different subdomains of the ER. We determined that running the cell homogenate on a discontinuous (5 %, 10 %, 15 %, 20 %, and 25 %) optiprep gradient would give us the best results in terms of separating different subdomains of the endoplasmic reticulum. The entire gradient was split into a total of six fractions to be run on SDS-PAGE with the top fraction (fraction 1) to be in the range of 5 % and the lowest fraction (fraction 6) in the range of 25 %. From using marker enzymes, we determined that we would be able to detect Golgi membranes in fraction 2 (shown by the protein βCOP, a component of non-clathrin-coated vesicles), and ERGIC (ER-Golgi intermediate compartment) membranes in fraction 3. Optiprep gradients separate ER membranes into fractions 4 to 6. In fraction 4, we detected mostly markers of the rough ER (rER), shown by the rER marker eIF2α (eukaryotic translation initiation factor), whereas in fraction 6 we detected markers of the MAM

(ACAT1, Acetyl-Coenzyme A acetyltransferase 1). Optiprep gradients were not able to completely separate the membranes of the ER from the membranes of mitochondria, which are found in the 6th fraction (detected by the protein Complex II). Additionally, fraction 1 contains a variety of different materials such as cytosolic proteins or proteins localized to the plasma membrane and endosomes. To examine Ero1α fractionation, HEK293T cells were used rather than HeLa cells which were used for the immunofluorescence studies in 3.1, because the expression level of Ero1α in HeLa cells was too low to allow for accurate determination of its distribution on our gradients. The majority of Ero1α to be located in fractions that co-migrate with markers of the MAM (fractions 5 and 6), rather than in other domains of the ER (Figure 3.2) which is consistent with our immunofluorescence data.

3.3 Subfractionation of ER and mitochondrial proteins

The results had shown so far that the ER protein Ero1α was targeting to a subdomain of the ER, the MAM. In order to examine the significance of these results, I next aimed to examine the localization of other ER-resident proteins on optiprep gradients, and compared these to that of Ero1α.

I analyzed a couple of different proteins and started with proteins that localized to mitochondria. The mitochondrial Complex II, for example, was indeed localizing only to the mitochondrial fraction (fraction 6) on the optiprep

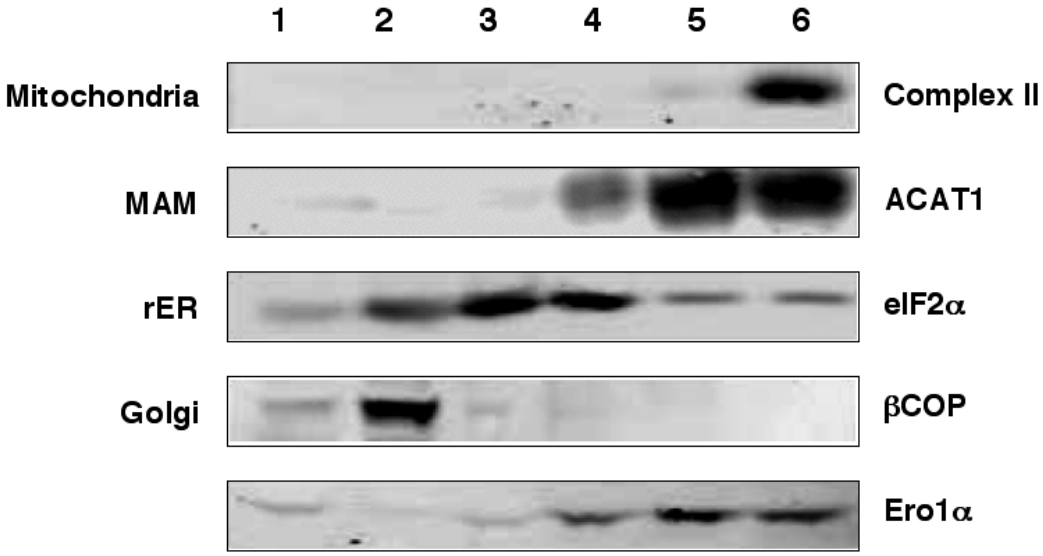

Figure 3.2: Ero1α co-fractionates with mitochondria and ACAT1, a MAM marker. HEK293T cell homogenates were fractionated on a discontinuous 5-25% optiprep gradient. Marker proteins indicate mitochondria (Complex II), MAM (Acat1), rER (eIF2α), and Golgi (βCOP).

gradients. The two GTPases mitofusin 1 & 2 (Mfn1 & 2 are required for mitochondrial fusion) were also found in fraction 6. These results could in principle mean that some Ero1α localizes to mitochondria as well. I tested for that possibility by digesting Ero1α with endoglycosidase endoH. This experiment showed that all of Ero1α could be digested by endoH, indicating that all of Ero1α resides in the ER (data not shown).

The chaperones BiP (Grp78) and calreticulin (CRT) both had a rather widespread fractionation pattern, which was also the case for PDI (Figure 3.3), consistent with their important role in oxidative protein folding throughout the ER. ERp44 on the other hand was exclusively found in fraction 3 which I had determined to be membranes of the ERGIC (data not shown). Another ER protein, calnexin (CNX), did not localize the same way that CRT, BiP and PDI did, but instead showed the same MAM targeting pattern like Ero1α. This distinct calnexin distribution was previously observed (Myhill *et al.* 2008) and therefore validates my results.

3.4 The effect of ER and mitochondrial stress reagents

Thapsigargin blocks the uptake of calcium by the ER SERCA pumps (sarcoplasmic and endoplasmic reticulum Ca^{2+}-ATPase). This blockage causes a disruption of ER calcium homeostasis, leading to the malfunction of ER-localized protein folding. Tunicamycin on the other hand, mimics the structure of UDP-*N*-

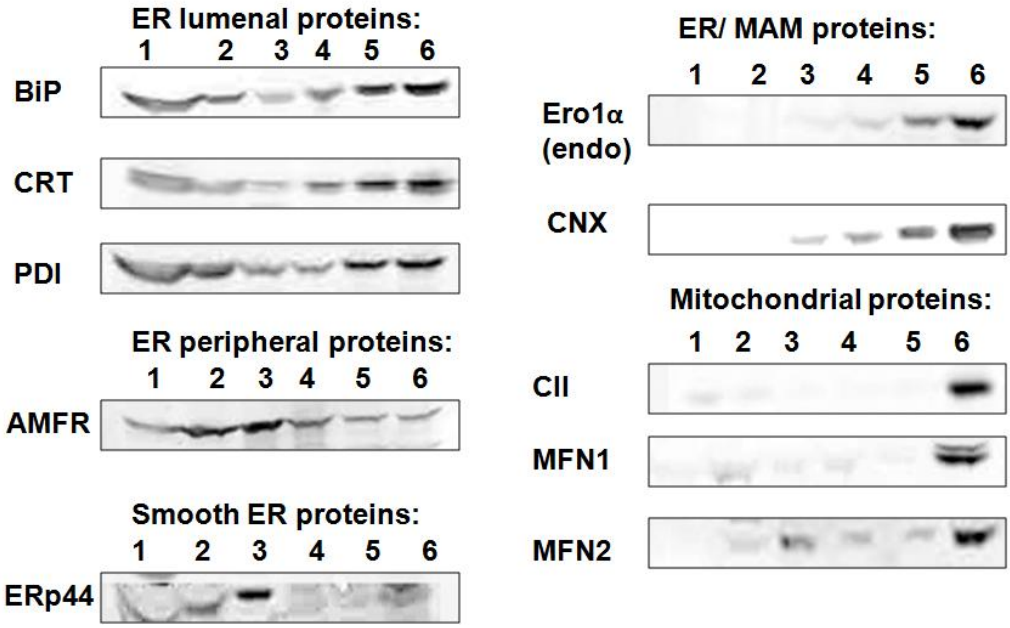

Figure 3.3: Other ER and mitochondrial proteins and their localization on a gradient. HEK293T cell homogenates were fractionated on a discontinuous 5-25% optiprep gradient. BiP, CRT and PDI represent ER luminal proteins. Mitochondrial proteins are Complex II (CII), Mitofusin 1 and 2 (MFN1/2). ERp44 is a protein found in the ERGIC and AMFR an ER peripheral protein. Ero1α and Calnexin (CNX) are both found on the MAM. All antibodies used were against the endogenous proteins.

acetylglucosamine and hence blocks the first step of the process of glycosylation. I hypothesized that the administration of drugs such as thapsigargin and tunicamycin could change Ero1α's targeting to the MAM if its localization to subdomains of the ER depends on ongoing oxidative protein folding. A disruption of the normal distribution of Ero1α would likely require an alteration of the ER redox state, since reducing conditions within the ER lead to the release of Ero1α from the ER (Otsu *et al.* 2006). Interestingly, it had been recently shown that the administration of tunicamycin results in a general alteration of the ER redox state (Merksamer *et al.* 2008), providing further support that the administration of tunicamycin could alter the intra-ER distribution of Ero1α, given that our hypothesis is correct. However, as shown in Figure 3.4, thapsigargin and tunicamycin both caused no change of localization of Ero1α.

Because we had found that Ero1α localizes to the vicinity of mitochondria and because its function may depend on the import of FAD from mitochondria, I next aimed to investigate whether mitochondrial function could influence the localization of Ero1α. Therefore I investigated the effect of the specific mitochondrial toxins oligomycin, rotenone, and antimycin, all of which interfere with the mitochondrial electron transport chain. Oligomycin is an inhibitor of ATP synthesis by blocking the proton channel that allows for the conversion of ADP into ATP (Gong and Agani 2005). Rotenone is a chemical that will essentially prevent the electron transfer from the Fe-S center to ubiquinone (Nicholls 2008). Antimycin acts similar to rotenone as it blocks also the electron

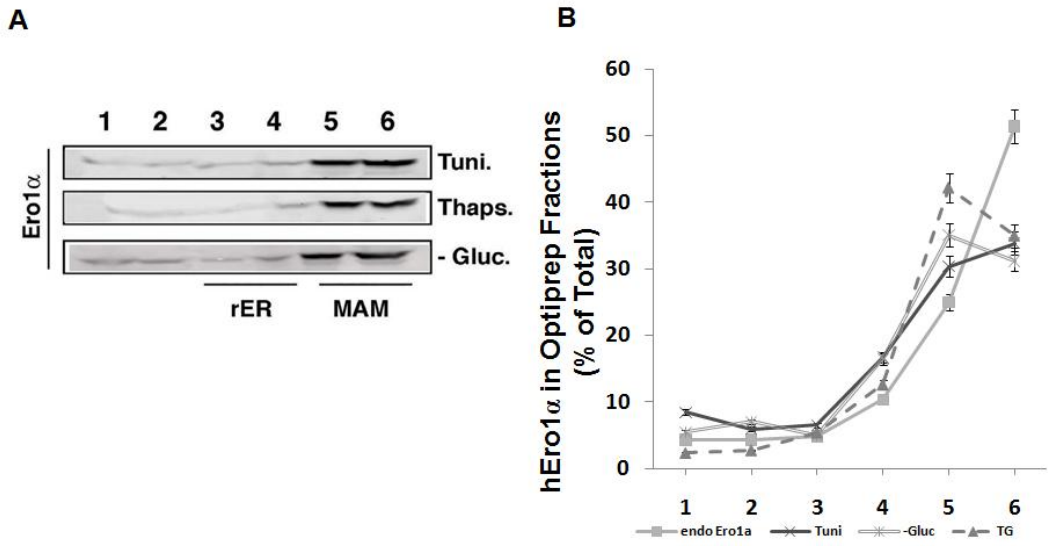

Figure 3.4: Interfering with stress agents that target the ER and the glucose metabolism. HEK293T cells were grown on 15cm Petri dishes for approximately 3 to 4 days. Cells were harvested and the homogenates were fractionated on a discontinuous 5-25% optiprep gradient. Prior to harvesting, all cells except for the controls were treated for 2 h with either 1μM thapsigargin (TG), 10μM tunicamycin (Tuni), or Glucose-free-medium (-Gluc) and left in the cell culture incubator (37˚C). Samples were run on SDS-PAGE and western blots were performed using antibody against endogenous Ero1α (see panel A). Panel B shows the quantification of the distribution of Ero1α upon treatment with the stress agents.

transfer but in this case from cytochrome b to cytochrome c_1 (Skulachev 1998). Although all of these treatments lead to the interference at various steps of oxidative phosphorylation, our experiments showed that none of these three blockers of mitochondrial oxidative phosphorylation had any effects on the localization of Ero1α (Figure 3.5).

3.5 The effect of strong reducing agents such as 2ME and DTT

Since the treatment of ER and mitochondrial stress reagents did not alter the localization of Ero1α, we next wanted to determine if β-mercaptoethanol (2ME) and dithiothreitol (DTT) would result in a change of localization. 2ME and DTT are both strong reducing agents and break existing disulfide bonds. Anelli *et al* (Anelli *et al.* 2002) have demonstrated that the treatment with DTT alters the abundance of the two isoforms of Ero1α, Ox1 and Ox2. These two monomeric redox isoforms were initially identified in transfected mammalian cells (Benham *et al.* 2000). They are thought to be necessary to change Ero1α's conformation as it accepts electrons from PDI and then again when it shuttles the electrons to FAD (Anelli *et al.* 2002). It was found that under resting conditions, Ox2 prevailed, whereas the administration of DTT caused an increase in Ox1 over Ox2. Furthermore, incubating the cells with reducing agents caused the secretion of overexpressed Ero1α (Otsu *et al.* 2006) because the addition of the reducing agent DTT caused the disassociation of Ero1α and ERp44 that retains Ero1α in the ER (Anelli *et al.* 2003). We hence wanted to determine if the addition of several ER-

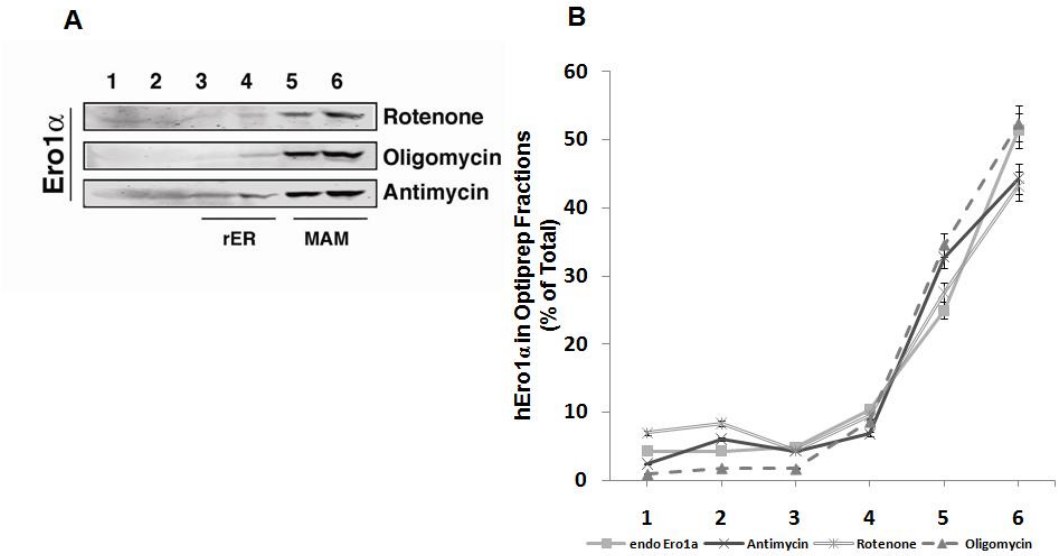

Figure 3.5: Interfering with stress agents that target mitochondrial metabolic processes. HEK293T cells were grown on 15cm Petri dishes for approximately 3 to 4 days. Cells were harvested and the homogenates were fractionated on a discontinuous 5-25% optiprep gradient. Prior to harvesting, all cells except for the controls were treated for 2 h with 10 μM oligomycin, 1 μM rotenone, or 10 μM antimycin and left in the cell culture incubator (37°C). Samples were run on SDS-PAGE and western blots were performed using antibody against endogenous Ero1α. Panel A shows the performed western blot. Panel B shows the quantification of the distribution of Ero1α.

stress inducing drugs could possibly change the location of endogenous Ero1α as well and aimed to test these findings on an optiprep gradient using only endogenously expressed proteins instead of overexpressed ones.

We therefore treated non-transfected HEK293T cells for 2 h with 5 mM DTT and 5 mM 2ME, homogenized the cells and loaded them onto gradients. As shown in Figure 3.6, both 2ME and DTT lead to a shift of Ero1α towards the 1st and 2nd fractions.

Figure 3.7 illustrates the distribution of Ero1α on an optiprep gradient upon treatment with the two reducing agents DTT and 2ME. The control peaks in fraction 6, while the amount of Ero1α after DTT/2ME treatment decreases by 50 % or even more than that in the case of 2ME in fraction 6. The graph in this Figure also demonstrates adequately the distinct increase of Ero1α seen in fractions 1 and 2 after exposure to either DTT or 2ME which is observed in Figure 3.6.

3.6 Hypoxia and its effect on the localization of Ero1α

As molecular oxygen appears to be the terminal electron acceptor during oxidative protein folding involving Ero1α in eukaryotes, we were intrigued to know if a hypoxic environment would possibly change the localization of Ero1α as a result of malfunctioning. Additionally, the expression of Ero1α is regulated

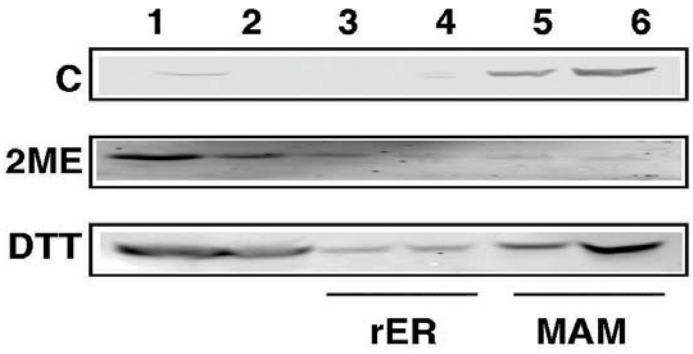

Figure 3.6: Interfering with strong reducing agents such as 2ME and DTT. HEK293T cells were grown on 15cm Petri dishes for approx. 4 d. Cells were harvested and the homogenates were fractionated on a discontinuous 5-25 % optiprep gradient. Prior to harvesting, all cells except for the controls were treated for 2 h with 5 mM 2ME or 5 mM DTT and left in the cell culture incubator (37°C). Samples were run on SDS-PAGE and western blots were performed using antibody against endogenous Ero1α.

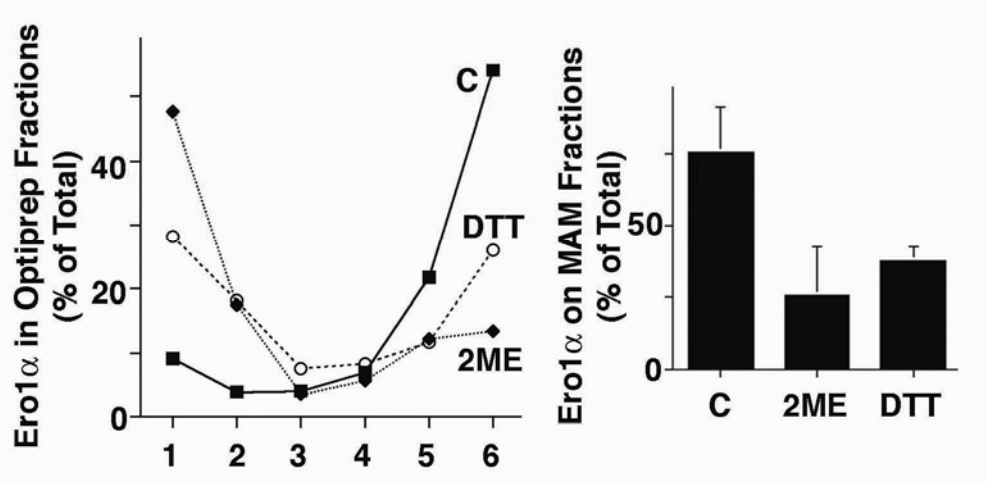

Figure 3.7: The distribution of Ero1α upon treatment with DTT and 2ME. In this graph, the amounts in the various fractions were quantified and blotted. The total amount of Ero1α in fraction 1 after treatment with either DTT or 2ME increases drastically whereas total amounts of Ero1α on the MAM after treatment decrease by approximately 50 %.

by HIF1α (Gess *et al.* 2003) Furthermore, oxygen depletion causes a drastic interference with mitochondria and could thus affect Ero1α in that regard. I therefore treated HEK293T cells for 2 h in a hypoxic environment containing 1 % oxygen (normoxia = 21 % O_2). On a 6-fraction gradient (optiprep), I observed a significant shift of Ero1α from the MAM towards the first two fractions (Figure 3.8), indicating that the incubation of HEK293T cells in a hypoxic environment caused the relocalization of Ero1α. Our next step was to determine the time point at which Ero1α starts shifting away from the MAM under hypoxic conditions. HEK293T cells were incubated in a hypoxic environment containing 1 % oxygen and were lysed after 15 min, 30 min, 1 hr, 2 h, 8 h, and 16 h. The lysates were loaded onto the optiprep gradients. As shown in Figure 3.8, Ero1α already starts shifting towards the light membranes after only 15 min and 1 % oxygen. Extended incubation (up to 16 h) in a hypoxic environment results in near complete shift of Ero1α away from the MAM. When exposed for 16 h to the hypoxic environment, Ero1α seemed to have vanished from the MAM fraction and most of it was in fraction 1 (Figure 3.8). We aimed to test if this effect was seen only with Ero1α or also with other proteins. Interestingly, this shift of localization upon incubation in a hypoxic environment was specific, since it was only seen with Ero1α and not other ER-resident proteins such as calnexin and BiP (Figure 3.10).

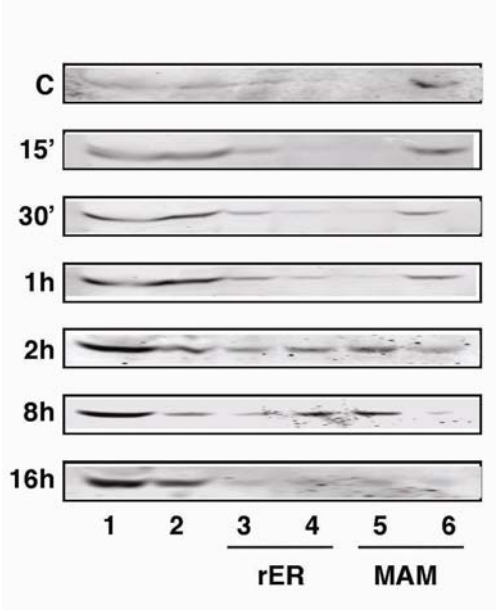

Figure 3.8: Hypoxia and Ero1α. HEK293T cells were grown in 15 cm petri dishes for approximately 3 to 4 d. Cells were harvested and the homogenates were fractionated on a discontinuous 5-25 % optiprep gradient. Prior to harvesting, all cells except for the controls were incubated for the amount indicated with 1 % oxygen in a hypoxic chamber at 37°C. Samples were run on SDS-PAGE and western blots were performed using antibody against endogenous Ero1α.

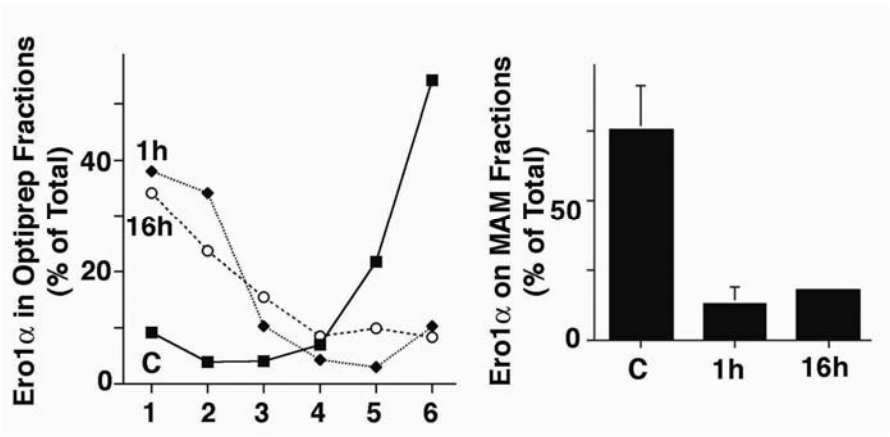

Figure 3.9: The distribution of Ero1α after hypoxic treatment. In the graphs, the amounts in the various fractions were quantified and blotted. The hypoxic treatment for 1 h and 16 h caused a drastic increase of total expression levels Ero1α in fractions 1 and 2 versus the control. The second panel indicates a 16 fold decrease of Ero1α on the MAM after treatment with hypoxia.

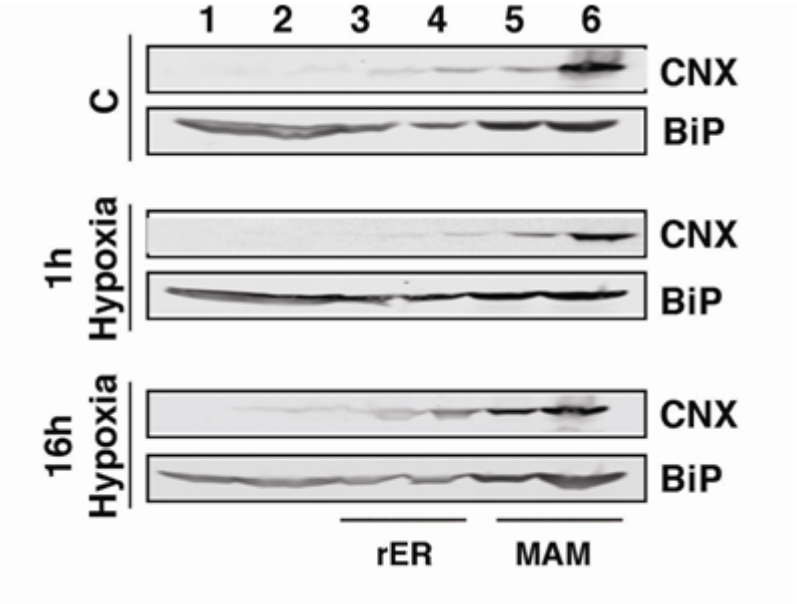

Figure 3.10: Hypoxia and the ER-resident proteins calnexin (CNX) and BiP. HEK293T cells were grown on 15cm petri dishes for approximately 3 to 4 d. Cells were harvested and the homogenates were fractionated on a discontinuous 5-25 % optiprep gradient. Prior to harvesting, all cells except for the controls were incubated for the amount indicated with 1 % oxygen in a hypoxic chamber at 37°C. Samples were run on SDS-PAGE and western blots were performed using antibody against endogenous calnexin and BiP.

3.7 Ero1α is upregulated in melanoma tissue and promotes the secretion of VEGF in HeLa cells

Ero1α has previously been demonstrated to be upregulated in certain tumor tissues (Francis *et al.* 2007). We therefore wanted to test to which extent this was also valid in randomly chosen melanoma samples. (These experiments were carried out by Kevin Gesson, University of Alberta, Dr. Simmen's Laboratory).

May *et al.* (2004) have provided genetic evidence that the upregulation of Ero1α by hypoxia is controlled by the hypoxia-inducible-factor 1 (HIF1) (May *et al.* 2004). Interestingly, they have also shown that a hypoxic environment causes the induction of Ero1α mRNA in human tumors. Their experiments showed that VEGF (vascular endothelial growth factor) secretion depends on Ero1α. This was confirmed by using siRNA to knockdown Ero1α which resulted in a striking decrease in the secretion of VEGF. For that reason, we obtained melanoma tissue for analysis from the Alberta Tumor Bank to verify if this was also the case for melanoma samples. Figure 3.11 demonstrates that Ero1α is indeed strongly upregulated in all our 10 melanoma tissue samples whereas the control which represents normal human skin tissue (obtained from Leinco Technologies, St. Louis, Missouri) shows next to no expression of Ero1α.

Kevin Gesson has shown that the overexpression of Ero1α in HeLa cells under hypoxic conditions causes an increase in the production of VEGF (Figure 3.12). Interestingly, a VEGF secretion of untransfected HeLa cells that were

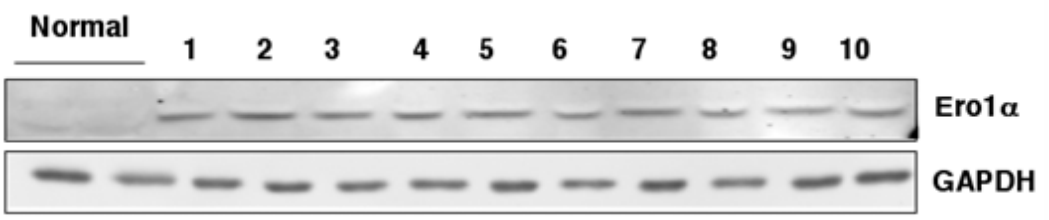

Figure 3.11: The upregulation of Ero1α in melanoma tissue. 50 μg of each melanoma tissue lysate was loaded (numbered 1-10) as well as 50 μg of normal human skin tissue. Samples were run on SDS-PAGE and western blots were performed using antibody against endogenous Ero1α and GAPDH. (Work from Kevin Gesson, Simmen Lab, unpublished data).

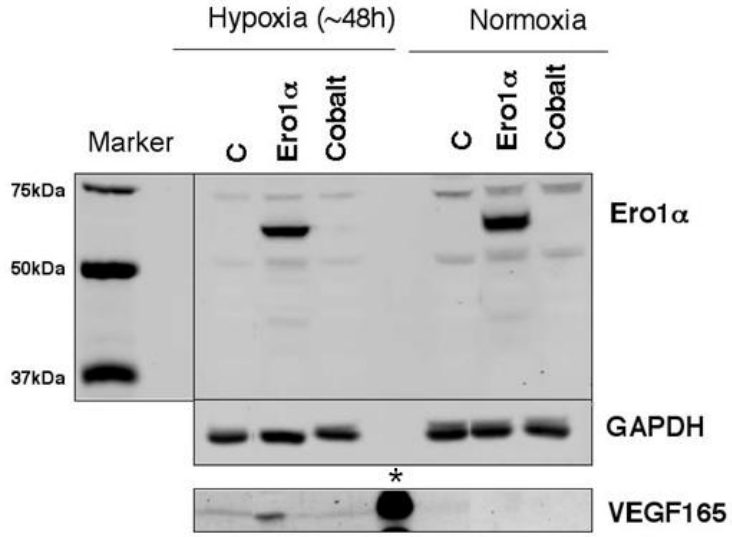

Figure 3.12: The secretion of VEGF from HeLa cells is regulated by Ero1α. HeLa cells were transfected with Ero1α-myc or left untransfected (control and cobalt lanes). The cells were exposed to hypoxia for 48 h and lysed. The supernatant was collected and a secretion assay was performed to test for the secretion of VEGF. Cobalt chloride which mimics hypoxia was added to untransfected HeLa cells. Samples were run on SDS-PAGE and western blots were performed using antibody against myc, GAPDH and VEGF. The asterix indicates an unspecific band. (Work from Kevin Gesson, Simmen Lab, unpublished data).

treated with $CoCl_2$ (mimics hypoxia to some extent) was not observed (Figure 3.12). Further tests should verify if the chemical inducer of hypoxia, $CoCl_2$, was indeed working or if higher concentrations are required to induce proper secretion of VEGF.

3.8 Analysis of Ero1α-mutants

The retention of Ero1α on the MAM could be mediated by several different factors. One possibility could lie in the interaction with other ER-resident proteins such as PDI or ERp44; both of which have been shown to form mixed disulfides with Ero1α (Benham *et al.* 2000; Anelli *et al.* 2002). Therefore, the appropriate methodology to study this hypothesis is to perform point mutations in certain cysteine residues of Ero1α. In order to narrow down the sequence region of Ero1α that is involved in the localization of this oxidoreductase to the MAM, we decided to analyze a series of deletion mutants that span almost the entire sequence of Ero1α. Figure 3.13 shows all the deletion mutants that were constructed and indicates which specific cysteine residues affected by the deletion. The deletion mutants generally lack one or two cysteine residues. The following lists the amino acid sequence deletion and the corresponding cysteine residue(s): (Δ33-50; C35 C37,C46, C48), (Δ86-95; C94), (Δ96-115; C99, C104), (Δ115-155; C131), (Δ185-209; C208), (Δ238-271; C241), (Δ303-324), (Δ325-353), (Δ354-384), (Δ389-403), (Δ404-420), (Δ439-469), (Δ159-171; C166). Additionally, the mutants Δ185-209 and Δ238-271 both have a

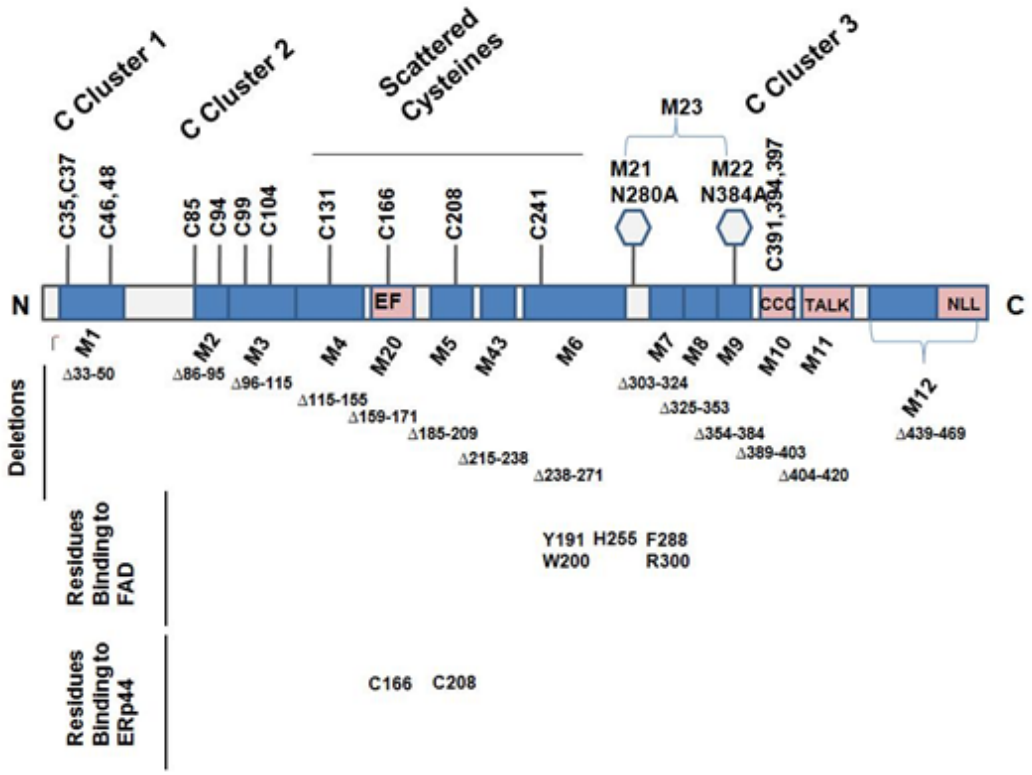

Figure 3.13: Overview of Ero1α with its cysteine clusters. Schematic lists all cysteine residues in wild type Ero1α and shows deletion mutants with blue boxes. All mutants start with an 'M' followed by a number. Hexagons indicate glycosylation sites. The cysteines C166 and C208 are required to bind ERp44. The residues Y191, W200, H255, F288 and R300 are responsible for the proper binding with FAD.

partial deletion of the FAD binding sites (FAD binds to Ero1α at Y191, W200, H255, F283, and R286). Mutant Δ159-171 lacks its EF-binding domain that contains cysteine 166 which is required for the binding of ERp44. Mutant Δ389-403 lacks all three cysteines C391, C394, and C397 which are necessary for transferring electrons onto FAD. Δ439-469 is missing a large part of its C-terminus. The Mutants N280A and N384A are both point mutations that lack the glycosylation sites, respectively. N280A/N384A contains two point mutations in both glycosylation sites.

3.8.1 Analysis of the Ero1α-mutants

Because the overexpression of Ero1α in HEK293T cells led to a distribution on the gradient that did not match the endogenous protein, I switched to HeLa cells that had a lower transfection efficiency, resulting in a distribution of overexpressed Ero1α that resembled the endogenous protein distribution. The mutants listed in Figure 3.13 were hence analyzed in HeLa cells using our 6-fraction optiprep-gradient to determine Ero1α's retention motif to the MAM. HeLa cells were transiently transfected with Metafectene and lysed/homogenized two days following transfection. Figure 3.14 shows both endogenous Ero1α in HEK293T cells and the overexpressed Ero1α-myc in HeLa cells to confirm similar patterns of localizations.

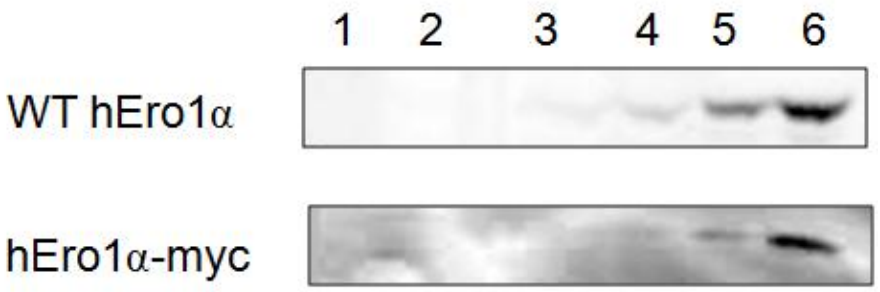

Figure 3.14: WT Ero1α vs. OE Ero1α-myc. HEK293T/HeLa cells were grown on 15cm Petri dishes for approximately 3 to 4 days. Cells were harvested and the homogenates were fractionated on a discontinuous 5-25% optiprep gradient. Samples were run on SDS-PAGE and western blots were performed using antibody against endogenous Ero1α and against myc.

The analysis of the following mutants did not reveal any change of the localization of Ero1α: Δ33-50, Δ86-95, Δ96-115, Δ115-155, Δ215-238, Δ303-324, Δ325-353, Δ354-384, Δ389-403, Δ404-420, Δ439-469 (data not shown). There were however a number of mutants that did seem to affect the localization of Ero1α. These were the FAD mutants Δ185-209 and Δ238-271 that lack a portion of the FAD-binding sites: Δ185-209 misses Y191 and W200, Δ238-271 lacks H255. In Figure 3.15, it is obvious that both these mutants cause a significant change of localization of Ero1α on the gradient towards the lighter membranes.

The ER protein ERp44 has been shown to form mixed disulfides with Ero1α. As a consequence, this interaction could be responsible for Ero1α's retention to the MAM. For that reason, the mutant Δ159-171 was constructed. This mutant lacks the entire EF-binding-domain which contains the cysteine C166, one of two that are required for the binding with ERp44 (Figure 3.13). As this mutant is expected to no longer bind calcium but also to inhibit interactions with ERp44, this could ultimately have multiple effects on Ero1α. Interestingly, this mutant shows a distinct shift away from the MAM towards other domains of the ER (Figure 3.16). This could suggest a potential retention motif for Ero1α. Conversely, this mutant lacks only one of the two cysteine residues required for forming mixed disulfides with ERp44. At this point, it is necessary to construct one more point mutant (C166A and C208A) to validate our findings. In addition, the effect of the non-existing calcium binding site on Ero1α needs further testing. This could give more insight as to why this EF-hand is important for Ero1α.

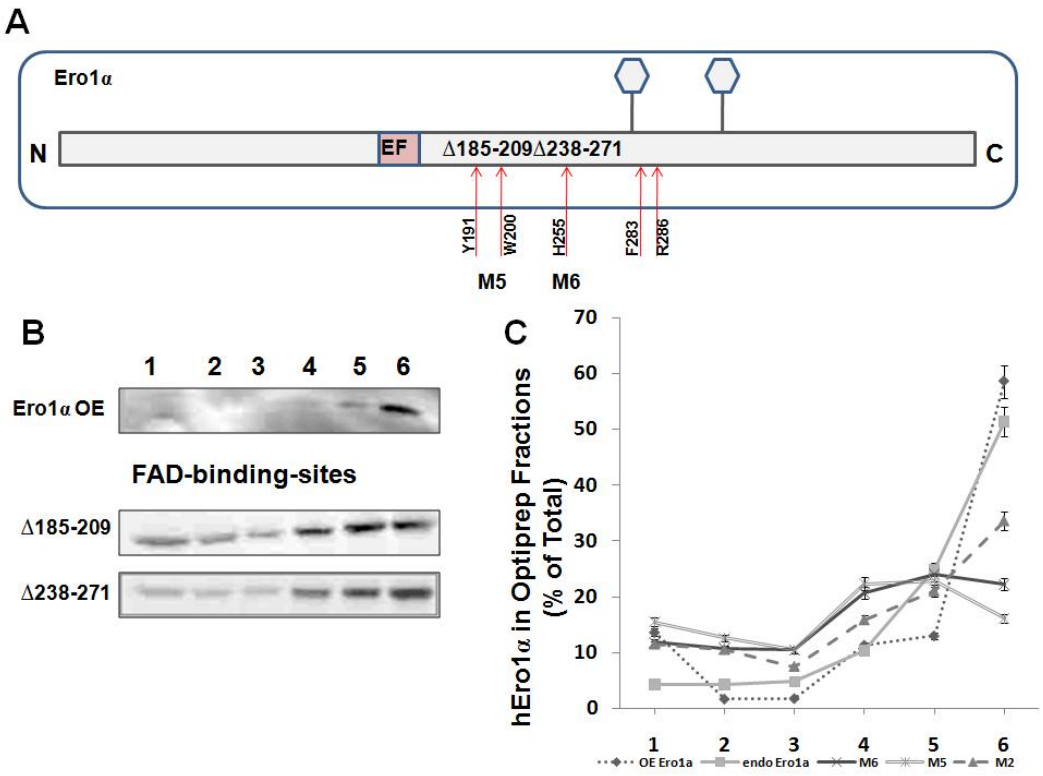

Figure 3.15: Analysis of Ero1α mutants Δ185-209 and Δ238-271. Schematic shows Ero1α's sequence with the red arrows pointing out where FAD usually binds to Ero1α. There are 5 FAD binding sites: Y191, W200, F283, R286, H255. Mutant M5 lacks part of the sequence at 185-209 and M6 lacks 238 to 271. Panel A: The last 2 arrow bars indicate FAD binding sites F283 and R296 (Mutants have not been made yet for these sites). Hexagons indicate glycosylation sites. Panel B: HeLa cells were grown on 15cm Petri dishes for approximately 3 to 4 days. Cells were harvested and the homogenates were fractionated on a discontinuous 5-25% optiprep gradient. Samples were run on SDS-PAGE and western blots were performed using antibody against myc. Panel C: Controls are Ero1α endogenous, overexpressed (myc-tag) and mutants M2 (negative control). In this graph, the amounts in the various fractions were quantified and normalized to 100% and graphed. Wild type Ero1α is mostly found the last 2 fractions (MAM). Mutants M5 and M6 show a drastic decrease (approx. 50% less than the control) in MAM targeting and seem to have an increase in the ER (fraction 4).

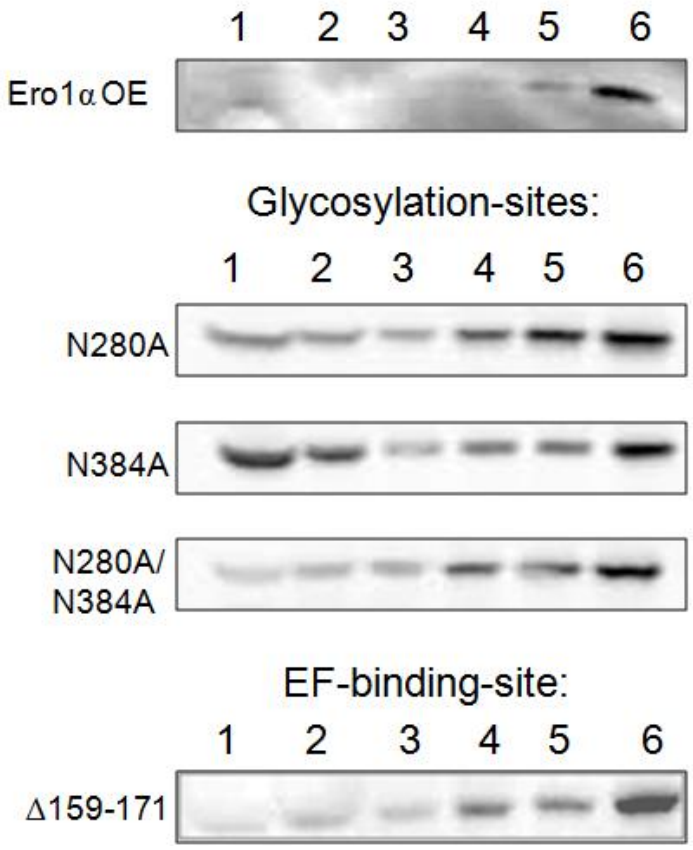

Figure 3.16: Analysis of Ero1α mutants N280A, N384A, N280A/N384A and Δ159-171. HeLa cells transfected with the indicated plasmids. The homogenates were fractionated on a discontinuous 5-25% optiprep gradient. Samples were run on SDS-PAGE and western blots were performed using antibody against myc-tag.

I have pointed out previously that Ero1α contains two glycosylation sites located at N280 and N384 in its sequence. Glycosylation is a crucial event for protein folding which could mean that the mutation of Ero1α in its glycosylation sites can possibly result in a misfolded Ero1α which also could be mislocalized. Consequently, we wanted to test whether the glycosylation sites of Ero1α played a role in its localization. For this reason, the following point mutants were created: N280A, N384A and N280A/N384A. Figure 3.16 demonstrates how the localization of Ero1α is changed upon mutating the specific amino acid for the glycosylation site(s). We can observe a significant shift towards the lighter membranes which are the upper fractions towards the left side of the gradient.

In summary, these findings confirm what we have found previously with the treatments of both DTT and 2ME. As the treatment of these chemicals restrain Ero1α from forming mixed disulfides with ERp44. Additionally, the binding of Ero1α to FAD could be a possible retention motif that targets Ero1α to the MAM.

Chapter 4 – Discussion

The ER luminal protein, Ero1α, is a key player in oxidative protein folding involving the protein disulfide isomerase PDI. Our immunofluorescence experiments revealed that Ero1α localizes to a specific ER-domain, called the mitochondria-associated-membrane (MAM). The MAM is important for the redox-dependent interaction of ERp44 with the IP3 receptor, for example. We have seen that Ero1α co-localizes with both mitochondria and the ER, represented by the ER luminal protein PDI (Figure 3.1). The biochemical analysis confirmed this finding. However, rather than being enriched in fractions 3 or 4 (smooth and rough ER) on the optiprep gradient, Ero1α peculiarly fractionates to fractions 5 and 6, where we also find ACAT1 (Acetyl-Coenzyme A acetyltransferase 1), a well established marker for the MAM.

To begin with, we wanted to examine mitochondrial proteins on optiprep gradients. Complex II (CII), also known as succinate dehydrogenase or succinate-coenzyme Q reductase, is part of the electron transport chain within mitochondria. We find CII solely in fraction 6 on optiprep gradients, marking it for mitochondria. Both mitofusin 1 and 2, two mitochondrial outer membrane proteins that mediate mitochondrial membrane dynamics, are exclusively found in fraction 6 as well. Calnexin is found primarily on the MAM together with Ero1α (Figure 3.3). We have previously shown that the amount of CNX on the MAM is around 2/3 of the total (Myhill *et al.* 2008). However, these results are also perplexing, as we know that calnexin plays an important role at the rER for newly synthesized polypeptide chains that enter the ER lumen.

The chaperone calreticulin (CRT) can be found in the rER and the ER-subdomain, the MAM, but also in the first two fractions (fractions 1 and 2), suggesting that calreticulin is not enriched in a particular domain of the ER. Interestingly, the other two luminal ER-proteins PDI and BiP show a similar pattern: most is found in fractions 5 and 6 (MAM), a bit less in 3 and 4 (sER and rER) and again slightly more in fractions 1 and 2 (fraction 2 = Golgi) (Figure 3.3). These patterns could be due to their high abundances within the cell or simply a result of the cell-homogenization-procedure. The homogenization could possibly break up organelles such as the ER, which would leave us with very light and small particles such as the endosomes which can form as a result of homogenization. These resulting endosomes can then end up in fraction 1 on our optiprep gradient due to their light weight.

Another marker, AMFR (Autocrine Motility Factor Receptor) (gp78), which contains a transmembrane domain has been shown to be associated with tumor metastasis (Fang *et al.* 2001). Fang *et al.* demonstrated that AMFR's ubiquitin ligase activity depends on its RING-finger domain. Figure 3.3 illustrates that the protein AMFR is found on the smooth ER and to some extent at the ERGIC (fractions 2 and 3) which is consistent with its association in ERAD. Another interesting result is that this protein was also found on tubules close to mitochondria which makes AMFR a particularly special case (Nabi *et al.* 1997).

Another ER protein shown in Figure 3.3 is ERp44, which is a soluble protein that contains an RDEL motif for retention and retrieval (Anelli *et al.*

2002). This thioredoxin family member (TRX) has been shown to be part of the ER calcium homeostasis mechanism. It regulates the IP3-receptor type I by direct interaction with its L3V (the channel domain of IP3R1 contains six transmembrane domains of which L3V is a subdomain) domain which results in the inhibition of the IP3R1 channel activity (Higo *et al.* 2005). It is also involved with the retention of several substrate proteins by forming mixed disulfides (Anelli *et al.* 2003; Fraldi *et al.* 2008). Figure 3.3 indicates that we find ERp44 in fraction 3 (smooth ER) on an optiprep gradient.

Taken together, this means that we are able to adequately separate different domains of the ER, as well as mitochondria and ERGIC/Golgi on our optiprep gradient.

We next demonstrated in Figure 3.4 that the administration of both tunicamycin and thapsigargin had no effect on the localization of Ero1α. Tunicamycin causes a block in glycosylation. However, it is important to note that this block will not only affect the glycosylation of Ero1α but all glycoproteins that are within the ER. Hence, the overall block of glycosylation will eventually result in the malfunctioning of protein folding which in turn triggers the unfolded protein response (UPR). Thapsigargin will inhibit the SERCA pumps (sarcoplasmic and endoplasmic reticulum calcium), blocking the ER from up taking calcium from the cytosol. The addition of thapsigargin to the cells, again will cause an overall increase of ER stress resulting in the upregulation of the

UPR. Given the results shown in Merksamer *et al* (2008) that show that tunicamycin administration causes a reduction of the ER environment, we were surprised not to see an effect of this drug on the localization of Ero1α. It is however possible that tunicamycin does not cause a complete reduction of disulfide bonds within the ER, this still allowing for the proper localization of Ero1α. Further experiments will have to be performed in order to show that the treatment of both thapsigargin and tunicamycin indeed caused ER stress. Measuring the splicing of the Xbp1 or examining the mRNA of CHOP for example could help determine the ER stress levels after the administration of either thapsigargin or tunicamycin.

Glycolysis is a well-known metabolic pathway in which glucose ($C_6H_{12}O_6$) is transformed into pyruvate ($C_3H_3O_3$). This process results in the release of energy in the form of ATP and NADH. Normal cells mainly use a process called mitochondrial oxidative phosphorylation to gain approximately 36 mol ATP/mol glucose of free energy (Vander Heiden *et al.* 2009). Very low oxygen concentrations allow the cell to switch from oxidative phosphorylation to anaerobic glycolysis. During anaerobic glycosylation, glucose is first transformed into pyruvate and then converted into lactate. These circumstances are not ideal for the cell but it is still able to produce roughly 2-4 mol ATP/mol glucose (Vander Heiden *et al.* 2009). Cancer cells on the other hand can readily switch from oxidative phosphorylation to aerobic glycosylation, even in the presence of oxygen. Additionally, it is important to mention that many ER chaperones get

induced in the absence of glucose which explains why many of them are named GRPs (Glucose-Regulated-Protein) (Lee 1992). It was important to determine if the localization of Ero1α was coupled to glycolysis. Therefore, the growth medium was changed to glucose-free medium and the cells were exposed to it for a total of 2 h. As demonstrated in Figure 3.4, the depletion of glucose in the medium caused a slight shift of Ero1α towards fractions 1 and 2. The change of localization of Ero1α could indicate that a switch from oxidative phosphorylation to aerobic glycosylation causes Ero1α to not function properly and eventually results in its secretion. This could mean that Ero1α requires a certain concentration of oxygen to operate and localize properly.

The depletion of glucose had shown a slight change in Ero1α's locations. The metabolic process of both aerobic and anaerobic glycosylation appears to occur within mitochondria. Therefore, it was important to test whether the intervention with other metabolic processes within mitochondria could have an additional effect on Ero1α. For this purpose, the chemical reagents antimycin, rotenone and oligomycin were administered to the cells for a total length of 2 h. Figure 4.1 shows where each of these three drugs targets the mitochondrial electron transport chain. Interestingly, as seen in Figure 3.5, none of these three drugs had any significant affect on Ero1α. There could be a slight decrease of

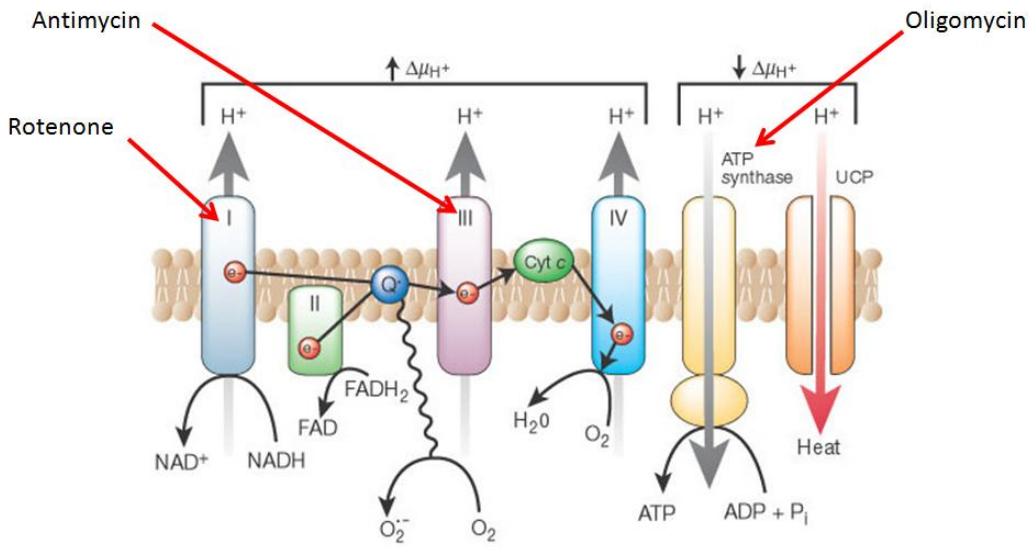

Figure 4.1: Interfering with stress agents that target mitochondrial metabolic processes. The schematic shows the mitochondrial electron transport chain and demonstrates where each drug is targeting. Rotenone prevents the electron transfer from the Fe-S center to ubiquinone (in blue: Q); Antimycin blocks the electron transfer from cytochrome b to cytochrome c_1 (shown in green); Oligomycin is an inhibitor of the ATP synthesis by blocking the proton channel that allows for the conversion of ADP into ATP. (Modified from Michael Brownlee *Nature*, 2001)

Ero1α in fractions 5 and 6 but this conclusion cannot be made at this point. In general rotenone, antimycin and oligomycin had no effect on the localization of Ero1α. This suggests that the mitochondrial electron transport chain has no effect on the retention of Ero1α to the MAM.

Anelli *et al* had demonstrated in 2002 that the reducing agent DTT (dithiothreitol) had a significant effect on Ero1α as it altered the amount of its two redox forms, Ox1 and Ox2. Reducing agents can disrupt existing disulfide bonds in proteins. Both 2ME and DTT were added to HEK293T cells for a total of 2 h. The effects on the localization of Ero1α of both 2ME and DTT are shown in Figure 3.6. 2ME is the stronger reducing agent of the two and caused a complete shift of Ero1α towards the first fraction (Figure 3.6). Almost no Ero1α remains at the MAM. DTT on the other hand caused a less intense effect as compared to 2ME. A significant amount of Ero1α is moved towards fractions 1 and 2 but a large quantity of Ero1α remained at the MAM (Figure 3.6 and 3.7). Why would a strong reducing agent as 2ME cause the complete depletion of Ero1α off the MAM? First of all, this suggests a total breakup of all disulfide bonds within the cell leading to cell death. To verify this, further experiments should prove whether certain apoptotic pathways are indeed upregulated upon the treatment with either DTT or 2ME and immunofluorescence might help in determining the state of the MAM. Another very useful tool can be electron microscopy in this case, in terms of the condition of the MAM.

Experiments using glucose-depleted medium gave little insight into the motif of Ero1α. As molecular oxygen is the terminal electron acceptor in oxidative protein folding, we sought to further investigate the role of oxygen in regards to Ero1α's localization. Therefore, we tested this by exposing the cells to a hypoxic environment with the oxygen levels not exceeding 1 %. The exposure of the cells to the hypoxic environment caused a significant shift of Ero1α away from the MAM (Figure 3.8). After 15 min of exposure, Ero1α first appears in the first two fractions but nonetheless remains on the MAM. The time course in Figure 3.8 shows that Ero1α starts coming off the MAM after 2 h of exposure when first signs of Ero1α appear in fractions 3 and 4 (sER and rER). After 8 h, not much is left of Ero1α on the MAM and 16 h of hypoxia reveal a complete loss of Ero1α on the MAM (Figure 3.8). The distribution of Ero1α on the gradient was analyzed in Figure 3.9. Here we can see that a 1 % oxygen environment caused a decrease of Ero1α initially found on the MAM from approximately 55 % to approximately 10 %. While the amount of Ero1α decreased on the MAM after 16 h of hypoxia, it is significantly increased in the first fraction. This is the first time that we have seen that Ero1α moves completely away from the MAM. Control cells showed approximately 10 % of Ero1α in fraction 1 while the cells exposed to 16 h of hypoxia showed an average of approximately 35 % in the same fraction (Figure 3.9).

In conclusion, it seems highly likely that molecular oxygen plays a major part in the retention mechanism of Ero1α on the MAM. If the cell encounters very low levels of oxygen over an extended period of time, mechanisms such as UPR

activation will be necessary for survival. Ero1α, together with its counterpart Ero1β would get upregulated as well. As oxygen levels are decreasing over time, the cell would then induce its apoptotic mechanisms as a result of prolonged stress. 16 h of low oxygen levels can certainly be seen as prolonged stress for the cell. Is the induction of apoptotic mechanisms responsible for Ero1α's release off the MAM or are there any other mechanisms that are accountable for what we have seen in Figure 3.8.

It is very important at this point that Ero1β be analyzed on an optiprep gradient. This could give us helpful insight into the localization mechanism of Ero1α. Unfortunately, the question whether hypoxia can lead to the secretion of Ero1α remains and we are not able to make any conclusions at this point. A secretion assay that confirms this would be necessary as the optiprep gradient cannot give us any information on that. The secretion assay would work as follows: cells ought to be exposed to the hypoxic environment for a set amount of time. The supernatant will then be collected and the proteins within can be precipitated using TCA precipitation. Limitations to this assay are the very low amounts of Ero1α expressed endogenously and Otsu *et al*. (2006) have only observed secretion of Ero1α under conditions of overexpression. Very large amounts of supernatant in the range of 20ml might be necessary to obtain sufficient amounts of Ero1α.

Furthermore, it is very important to mention that the exposure to the hypoxic environment only had an impact on Ero1α and not on other ER-resident

proteins such as calnexin and BiP which is demonstrated in Figure 3.10. Their initial pattern (as seen in the control) across the optiprep gradient was rather dispersed. This pattern remained after the exposure to the hypoxic environment regardless of the various time points, indicating that no shift away from the heavy membranes towards the light membranes was observed.

In addition, unpublished data by Kevin Gesson has shown that Ero1α is upregulated in melanoma tissue (Figure 3.11). As researchers are trying to find certain expression patterns among metastasizing tumors, this finding could undoubtedly be useful. Metastasizing tumors have been shown to be very aggressive and their prognosis is usually extremely discouraging. Ero1α is known to be upregulated under hypoxic conditions such as the ones encountered in tumors. A substantial analysis of both Ero1α and β in several metastasizing tumors could reveal whether hEro1 can serve as a possible marker for these tumors, given that they are undeniably upregulated in a variety of different tumors which has not been shown before.

The secretion of VEGF (Vascular Endothelial Growth Factor) has been shown to be tightly associated to hypoxia (Xie *et al.* 2004). VEGF is an important factor that stimulates the formation of new blood vessels under hypoxic conditions. The newly formed blood vessels can then ensure sufficient oxygen delivery to the tissue. We wanted to examine whether there was a link between the secretion of VEGF, hypoxia and endogenous Ero1α in HeLa cells. The Ero1α-myc tagged transfected cells were exposed to a hypoxic environment containing

1% oxygen for 48 h and additionally, non-transfected cells were exposed to $CoCl_2$ (mimicking the hypoxic effect). It was clearly demonstrated that the overexpression of Ero1α under hypoxic conditions caused an increase in the secretion of VEGF (Figure 3.12). The control does not show any levels of VEGF secretion under both hypoxic and normoxic conditions. Interestingly, the administration of $CoCl_2$ to untransfected HeLa cells showed no significant detection of VEGF secretion under normoxia (Figure 3.12). The chemical $CoCl_2$ is able to activate hypoxic signaling in cells by means of stabilizing HIF1α (Vengellur and LaPres 2004). Presumably, this suggests that only the overexpressed Ero1α in combination with hypoxia is capable of sufficiently secrete VEGF.

To further analyze possible retention motifs within the amino acid sequence of Ero1α, several truncation and point mutations were created resulting in numerous Ero1α-mutants. We were hoping that these mutants could give us more insight into Ero1α's retention motif to the MAM. The analysis of the mutants revealed that only 6 of them actually showed a change of localization of Ero1α. These mutants were the FAD-mutants Δ185-209 and Δ238-271 (Figure 3.15), the three glycosylation-site-point-mutants N280A), N384A and N280A/N384A (Figure 3.16) and last but not least the mutant Δ159-171, which lacks the EF-binding motif (Figure 3.16).

The mutants Δ185-209 and Δ238-271 both are truncation mutants where a part of the FAD-binding domain is deleted in each. The shift of Ero1α towards the rER and away from the ER-subdomain MAM seems significant and could be the result of several reasons. First and foremost, these truncations could very well cause a misfolding of Ero1α itself. It has been established previously that the FAD-binding domain in Ero1α is not only essential for the electron transfer from Ero1α to FAD but moreover is crucial for the stability of hEro1 to maintain protein-protein interactions (Dias-Gunasekara *et al.* 2006). This leads to our hypothesis that FAD is indeed involved in retaining Ero1α on the MAM. FAD initially is an outcome from the TCA cycle (Tri cyclic acid cycle) known to take place within mitochondria. FAD must then find means by which it can be shuttled into the ER lumen. To date, such a FAD-transporter has not yet been identified in mammals. Figure 4.2 demonstrates a proposed model of Ero1α-FAD interaction and visualizes the approximate amounts needed of each protein to make the entire process function properly. This could explain why the partial deletion of FAD -binding sites results in a mislocalization of Ero1α.

To verify the role of FAD in the retention of Ero1α to the MAM, further experiments are required. For one, it is necessary to create point mutations for all of the 5 FAD-binding sites (Y191, W200, H255, F283, and R286). It is obvious that a truncation mutant that lacks all 5 FAD-binding sites is impossible to construct as this would mean a depletion of 95 amino acids and would greatly jeopardize the proper folding and functioning of Ero1α. In addition, we conducted experiments with riboflavin-free medium, which did not yield reproducible results

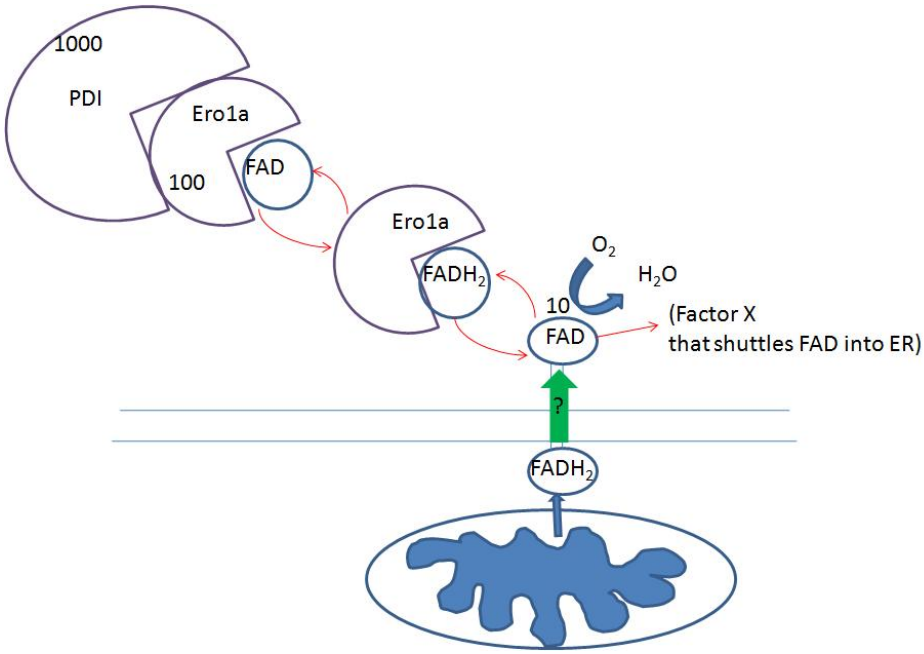

Figure 4.2: The interactions of PDI, Ero1α and FAD. This schematic illustrates the interactions of PDI (protein disulfide isomerase), Ero1α and FAD (flavin adenine dinucleotide). FAD is originally derived from the TCA cycle within mitochondria and is then shuttled into the ER lumen where is binds to Ero1α. Factor X (indicated by a green arrow) is responsible for transporting FAD into the ER. While approximately 100 Ero1α's can bind to and reoxidize some 1000 PDI, it requires only about 10 FAD molecules to recharge 100 Ero1α's.

(data not shown). Nevertheless, our data do seem to indicate that FAD plays a role to some extent to the localization of Ero1α.

It was shown with all three mutants that their overexpression changed the localization of Ero1α. In particular the mutant N384A showed a noteworthy increase in the first two fractions (Figure 3.16). N280A/N384A represents a mutant where both glycosylation sites are point mutated. Oddly enough, the expression pattern was not at all similar to that of either N280A or N384A. It was expected that N280A/N384A should be a summary of what was seen in both N280A and N384A but this seems not to be the case. Instead, N280A/N384A shows a drastic shift to fraction 4 (rER) (Figure 3.16). At this point it remains unclear as to what extent the role of the two glycosylation sites within Ero1α is important for the retention to the MAM. In addition, the analysis of Ero1β in this regard could prove insightful, but first, we would need to uncover to which ER subdomain Ero1β targets to. If it is not found on the MAM, then the difference in the number of glycosylation sites might indeed indicate a retention mechanism of Ero1α to the MAM.

The mutant Δ159-171 is a truncation mutant that lacks the EF -binding domain which is usually found in calcium-binding proteins to allow for the binding of calcium ions. Within this domain is the cysteine residue C166 which, together with cysteine C208 (Figure 3.14), is required to sufficiently bind Ero1α to ERp44. It has been shown previously that the formation of disulfide complexes with ERp44 and its substrate protein (such as Ero1α) can act as a retention

mechanism for ER luminal proteins. Interestingly, the lack of the EF -domain causes Ero1α to shift to fraction 4 (rER) but most of it remains on the MAM (Figure 3.17). Taken together, this suggests that the binding of Ero1α to ERp44 could possibly aid in retaining Ero1α on the MAM.

In conclusion, the analysis of our Ero1α's mutants has revealed several candidate sequences and motifs that could be important for the targeting of Ero1α to the MAM. Rather than one retention motif, there is a possibility of several components working together as a network that will eventually result in the retention of Ero1α to the MAM. However, my experiments have shown that molecular oxygen might be a major component that directs Ero1α's localization.

Chapter 5 – References

Achleitner, G., B. Gaigg, A. Krasser, E. Kainersdorfer, S. D. Kohlwein, A. Perktold, G. Zellnig and G. Daum (1999). "Association between the endoplasmic reticulum and mitochondria of yeast facilitates interorganelle transport of phospholipids through membrane contact." European Journal of Biochemistry **264**(2): 545-553.

Ameri, K. and A. L. Harris (2008). "Activating transcription factor 4." The International Journal of Biochemistry & Cell Biology **40**(1): 14-21.

Anelli, T., M. Alessio, A. Bachi, L. Bergamelli, G. Bertoli, S. Camerini, A. Mezghrani, E. Ruffato, T. Simmen and R. Sitia (2003). "Thiol-mediated protein retention in the endoplasmic reticulum: the role of ERp44." Embo J **22**(19): 5015-22.

Anelli, T., M. Alessio, A. Mezghrani, T. Simmen, F. Talamo, A. Bachi and R. Sitia (2002). "ERp44, a novel endoplasmic reticulum folding assistant of the thioredoxin family." Embo J **21**(4): 835-44.

Anelli, T. and R. Sitia (2008). "Protein quality control in the early secretory pathway." Embo J **27**(2): 315-27.

Anelli, T. and R. Sitia (2008). "Protein quality control in the early secretory pathway." EMBO J **27**(2): 315-327.

Appenzeller-Herzog, C., J. Riemer, B. Christensen, E. S. Sorensen and L. Ellgaard (2008). "A novel disulphide switch mechanism in Ero1[alpha] balances ER oxidation in human cells." EMBO J **27**(22): 2977-2987.

Bader, M., W. Muse, D. P. Ballou, C. Gassner and J. C. A. Bardwell (1999). "Oxidative Protein Folding Is Driven by the Electron Transport System." Cell **98**(2): 217-227.

Baksh, S., C. Spamer, C. Heilmann and M. Michalak (1995). "Identification of the Zn2+ binding region in calreticulin." FEBS Letters **376**(1-2): 53-57.

Baranska, J. (1980). "Phosphatidylserine biosynthesis in mitochondria from ehrlich ascites tumor cells." Biochimica et Biophysica Acta (BBA) - Lipids and Lipid Metabolism **619**(2): 258-266.

Bardwell, J. C. A. (2004). "The dance of disulfide formation." Nat Struct Mol Biol **11**(7): 582-583.

Benham, A. M., A. Cabibbo, A. Fassio, N. Bulleid, R. Sitia and I. Braakman (2000). "The CXXCXXC motif determines the folding, structure and stability of human Ero1-L[alpha]." EMBO J **19**(17): 4493-4502.

Benjamin, I. J. (2006). "Viewing a Stressful Episode of ER: Is ATF6 the Triage Nurse?" Circ Res **98**(9): 1120-1122.

Berg, J. M. (1990). "Zinc fingers and other metal-binding domains. Elements for interactions between macromolecules." Journal of Biological Chemistry **265**(12): 6513-6516.

Bernales, S. n., F. R. Papa and P. Walter (2006). "Intracellular Signaling by the Unfolded Protein Response." Annual Review of Cell and Developmental Biology **22**(1): 487-508.

Braakman, I., J. Helenius and A. Helenius (1992). "Role of ATP and disulphide bonds during protein folding in the endoplasmic reticulum." Nature **356**: 260 - 262.

Brahimi-Horn, C. and J. Pouyssegur (2006). "The role of the hypoxia-inducible factor in tumor metabolism growth and invasion." ELECTRONIC JOURNAL OF ONCOLOGY **93**(8): E73-80.

Brahimi-Horn, M., J. Chiche and J. Pouysségur (2007). "Hypoxia and cancer." Journal of Molecular Medicine **85**(12): 1301-1307.

Brenner, S., F. Jacob and M. Meselson (1961). "An Unstable Intermediate Carrying Information from Genes to Ribosomes for Protein Synthesis." Nature **190**(4776): 576-581.

Buck, T. M., C. M. Wright and J. L. Brodsky (2007). "The activities and function of molecular chaperones in the endoplasmic reticulum." Seminars in Cell & Developmental Biology **18**(6): 751-761.

Cabibbo, A., M. Pagani, M. Fabbri, M. Rocchi, M. R. Farmery, N. J. Bulleid and R. Sitia (2000). "ERO1-L, a Human Protein That Favors Disulfide Bond Formation in the Endoplasmic Reticulum." J. Biol. Chem. **275**(7): 4827-4833.

Christis, Lubsen and Braakman (2008). "Protein folding includes oligomerization; examples from the endoplasmic reticulum and cytosol." FEBS Journal **275**(19): 4700-4727.

Corbett, E. F., K. M. Michalak, K. Oikawa, S. Johnson, I. D. Campbell, P. Eggleton, C. Kay and M. Michalak (2000). "The Conformation of Calreticulin Is Influenced by the Endoplasmic Reticulum Luminal Environment." J. Biol. Chem. **275**(35): 27177-27185.

Corbett, E. F., K. Oikawa, P. Francois, D. C. Tessier, C. Kay, J. J. M. Bergeron, D. Y. Thomas, K.-H. Krause and M. Michalak (1999). "Ca2+ Regulation of Interactions between Endoplasmic Reticulum Chaperones." Journal of Biological Chemistry **274**(10): 6203-6211.

Csordas, G., C. Renken, P. Varnai, L. Walter, D. Weaver, K. F. Buttle, T. Balla, C. A. Mannella and G. Hajnoczky (2006). "Structural and functional features and significance of the physical linkage between ER and mitochondria." J. Cell Biol. **174**(7): 915-921.

Davenport, E. a. M., GJ and Davies,FE (2008). "Untangling the unfolded protein response." Cell Cycle **7**(7).

de Brito, O. M. and L. Scorrano (2009). "Mitofusin-2 regulates mitochondrial and endoplasmic reticulum morphology and tethering: The role of Ras." Mitochondrion **9**(3): 222-226.

Denko, N. C. (2008). "Hypoxia, HIF1 and glucose metabolism in the solid tumour." Nat Rev Cancer **8**(9): 705-713.

Depping, R., A. Steinhoff, S. G. Schindler, B. Friedrich, R. Fagerlund, E. Metzen, E. Hartmann and M. Köhler (2008). "Nuclear translocation of hypoxia-inducible factors (HIFs): Involvement of the classical importin [alpha]/[beta] pathway." Biochimica et Biophysica Acta (BBA) - Molecular Cell Research **1783**(3): 394-404.

Devlin, T., [ed.] (2002). "Textbook of Biochemistry with Clinical Correlations." Wiley-Liss(5th Edition).

Dias-Gunasekara, S. and A. M. Benham (2005). "Defining the protein-protein interactions of the mammalian endoplasmic reticulum oxidoreductases (EROs)." Biochem. Soc. Trans. **33**(Pt 6): 1382-1384.

Dias-Gunasekara, S., M. van Lith, J. A. G. Williams, R. Kataky and A. M. Benham (2006). "Mutations in the FAD Binding Domain Cause Stress-induced Misoxidation of the Endoplasmic Reticulum Oxidoreductase Ero1beta." J. Biol. Chem. **281**(35): 25018-25025.

Ellgaard, L. and L. W. Ruddock (2005). "The human protein disulphide isomerase family: substrate interactions and functional properties." EMBO Rep **6**(1): 28-32.

Fandrey, J. and M. Gassmann (2009). Oxygen Sensing and the Activation of the Hypoxia Inducible Factor 1 (HIF-1)– Invited Article. Arterial Chemoreceptors**:** 197-206.

Fang, S., M. Ferrone, C. Yang, J. P. Jensen, S. Tiwari and A. M. Weissman (2001). "The tumor autocrine motility factor receptor, gp78, is a ubiquitin protein ligase implicated in degradation from the endoplasmic reticulum." Proceedings of the National Academy of Sciences of the United States of America **98**(25): 14422-14427.

Fraldi, A., E. Zito, F. Annunziata, A. Lombardi, M. Cozzolino, M. Monti, C. Spampanato, A. Ballabio, P. Pucci, R. Sitia and M. P. Cosma (2008). "Multistep, sequential control of the trafficking and function of the multiple sulfatase deficiency gene product, SUMF1 by PDI, ERGIC-53 and ERp44." Hum. Mol. Genet. **17**(17): 2610-2621.

Francis, P., H. Namlos, C. Muller, P. Eden, J. Fernebro, J.-M. Berner, B. Bjerkehagen, M. Akerman, P.-O. Bendahl, A. Isinger, A. Rydholm, O. Myklebost and M. Nilbert (2007). "Diagnostic and prognostic gene expression signatures in 177 soft tissue sarcomas: hypoxia-induced transcription profile signifies metastatic potential." BMC Genomics **8**(1): 73.

Frand, A. R., J. W. Cuozzo and C. A. Kaiser (2000). "Pathways for protein disulphide bond formation." Trends in Cell Biology **10**(5): 203-210.

Frand, A. R. and C. A. Kaiser (1998). "The ERO1 Gene of Yeast Is Required for Oxidation of Protein Dithiols in the Endoplasmic Reticulum." Molecular Cell **1**(2): 161-170.

Freedman, R. B., A. D. Dunn and L. W. Ruddock (1998). "Protein folding: A missing redox link in the endoplasmic reticulum." Current Biology **8**(13): R468-R470.

Gess, B., K. Hofbauer, H. W. Roland, L. Christiane, E. M. Helmut and K. Armin (2003). "The cellular oxygen tension regulates expression of the endoplasmic oxidoreductase ERO1-L&#x03B1." European Journal of Biochemistry **270**(10): 2228-2235.

Goldberger, R. F., C. J. Epstein and C. B. Anfinsen (1964). "Purification and Properties of a Microsomal Enzyme System Catalyzing the Reactivation of Reduced Ribonuclease and Lysozyme." J. Biol. Chem. **239**(5): 1406-1410.

Gong, Y. and F. H. Agani (2005). "Oligomycin inhibits HIF-1{alpha} expression in hypoxic tumor cells." Am J Physiol Cell Physiol **288**(5): C1023-1029.
Gruber, C. W., M. Cemazar, B. Heras, J. L. Martin and D. J. Craik (2006). "Protein disulfide isomerase: the structure of oxidative folding." Trends in Biochemical Sciences **31**(8): 455-464.
Guth, S., C. Völzing, A. Müller, M. Jung and R. Zimmermann (2004). "Protein transport into canine pancreatic microsomes." European Journal of Biochemistry **271**(15): 3200-3207.
Hatahet and Ruddock (2007). "Substrate recognition by the protein disulfide isomerases." FEBS Journal **274**(20): 5223-5234.
Hayashi, T., R. Rizzuto, G. Hajnoczky and T.-P. Su (2009). "MAM: more than just a housekeeper." Trends in Cell Biology **19**(2): 81-88.
Hayashi, T. and T.-P. Su (2007). "Sigma-1 Receptor Chaperones at the ER-Mitochondrion Interface Regulate Ca2+ Signaling and Cell Survival." Cell **131**(3): 596-610.
Helenius, A. and M. Aebi (2004). "ROLES OF N-LINKED GLYCANS IN THE ENDOPLASMIC RETICULUM." Annual Review of Biochemistry **73**(1): 1019-1049.
Hetz, C., P. Bernasconi, J. Fisher, A.-H. Lee, M. C. Bassik, B. Antonsson, G. S. Brandt, N. N. Iwakoshi, A. Schinzel, L. H. Glimcher and S. J. Korsmeyer (2006). "Proapoptotic BAX and BAK Modulate the Unfolded Protein Response by a Direct Interaction with IRE1{alpha}." Science **312**(5773): 572-576.
Higo, T., M. Hattori, T. Nakamura, T. Natsume, T. Michikawa and K. Mikoshiba (2005). "Subtype-specific and ER lumenal environment-dependent regulation of inositol 1,4,5-trisphosphate receptor type 1 by ERp44." Cell **120**(1): 85-98.
Hirsch, C., R. Gauss, S. C. Horn, O. Neuber and T. Sommer (2009). "The ubiquitylation machinery of the endoplasmic reticulum." Nature **458**(7237): 453-460.
Hockel, M., K. Schlenger, B. Aral, M. Mitze, U. Schaffer and P. Vaupel (1996). "Association between Tumor Hypoxia and Malignant Progression in Advanced Cancer of the Uterine Cervix." Cancer Res **56**(19): 4509-4515.
Khalkhall, Z. and R. D. Marshall (1975). "Glycosylation of ribonuclease A catalysed by rabbit liver extracts." Biochem J. **146**(2): 299–307.
Kim, R., M. Emi, K. Tanabe and S. Murakami (2006). "Role of the unfolded protein response in cell death." Apoptosis **11**(1): 5-13.
Kramer, G., D. Boehringer, N. Ban and B. Bukau (2009). "The ribosome as a platform for co-translational processing, folding and targeting of newly synthesized proteins." Nat Struct Mol Biol **16**(6): 589-597.
Lai, E., T. Teodoro and A. Volchuk (2007). "Endoplasmic Reticulum Stress: Signaling the Unfolded Protein Response." Physiology **22**(3): 193-201.
Lee, A. S. (1992). "Mammalian stress response: induction of the glucose-regulated protein family." Current Opinion in Cell Biology **4**(2): 267-273.
Lee, K., R. A. Roth and J. J. LaPres (2007). "Hypoxia, drug therapy and toxicity." Pharmacology & Therapeutics **113**(2): 229-246.

Lees, W. J. (2008). "Small-molecule catalysts of oxidative protein folding." Current Opinion in Chemical Biology **12**(6): 740-745.

Levine, T. and C. Loewen (2006). "Inter-organelle membrane contact sites: through a glass, darkly." Current Opinion in Cell Biology **18**(4): 371-378.

Li, G., M. Mongillo, K.-T. Chin, H. Harding, D. Ron, A. R. Marks and I. Tabas (2009). "Role of ERO1-{alpha}-mediated stimulation of inositol 1,4,5-triphosphate receptor activity in endoplasmic reticulum stress-induced apoptosis." J. Cell Biol. **186**(6): 783-792.

Li, M., P. Baumeister, B. Roy, T. Phan, D. Foti, S. Luo and A. S. Lee (2000). "ATF6 as a Transcription Activator of the Endoplasmic Reticulum Stress Element: Thapsigargin Stress-Induced Changes and Synergistic Interactions with NF-Y and YY1." Mol. Cell. Biol. **20**(14): 5096-5106.

Lin, J. H., H. Li, D. Yasumura, H. R. Cohen, C. Zhang, B. Panning, K. M. Shokat, M. M. LaVail and P. Walter (2007). "IRE1 Signaling Affects Cell Fate During the Unfolded Protein Response." Science **318**(5852): 944-949.

Lin, J. H., H. Li, Y. Zhang, D. Ron and P. Walter (2009). "Divergent Effects of PERK and IRE1 Signaling on Cell Viability." PLoS ONE **4**(1): e4170.

Maattanen, P., G. Kozlov, K. Gehring and D. Thomas (2006). "ERp57 and PDI: multifunctional protein disulfide isomerases with similar domain architectures but differing substrate-partner associations." Biochem Cell Biol **84**(6): 881-889.

Mancini, R., M. Aebi and A. Helenius (2003). "Multiple Endoplasmic Reticulum-associated Pathways Degrade Mutant Yeast Carboxypeptidase Y in Mammalian Cells." J. Biol. Chem. **278**(47): 46895-46905.

Maxwell, P. H., M. S. Wiesener, G.-W. Chang, S. C. Clifford, E. C. Vaux, M. E. Cockman, C. C. Wykoff, C. W. Pugh, E. R. Maher and P. J. Ratcliffe (1999). "The tumour suppressor protein VHL targets hypoxia-inducible factors for oxygen-dependent proteolysis." Nature **399**(6733): 271-275.

May, D., A. Itin, O. Gal, H. Kalinski, E. Feinstein and E. Keshet (2004). "Ero1-L[alpha] plays a key role in a HIF-1-mediated pathway to improve disulfide bond formation and VEGF secretion under hypoxia: implication for cancer." Oncogene **24**(6): 1011-1020.

Merksamer, P. I., A. Trusina and F. R. Papa (2008). "Real-Time Redox Measurements during Endoplasmic Reticulum Stress Reveal Interlinked Protein Folding Functions." Cell **135**(5): 933-947.

Michalak, M., J. Groenendyk, E. Szabo, L. I. Gold and M. Opas (2009). "Calreticulin, a multi-process calcium-buffering chaperone of the endoplasmic reticulum." Biochem J **417**(3): 651-666.

Molinari, M., V. Calanca, C. Galli, P. Lucca and P. Paganetti (2003). "Role of EDEM in the Release of Misfolded Glycoproteins from the Calnexin Cycle." Science **299**(5611): 1397-1400.

Moreno-Sánchez, Rodríguez-Enríquez, Saavedra, Marín-Hernández and Gallardo-Pérez (2009). "The bioenergetics of cancer: Is glycolysis the main ATP supplier in all tumor cells?" BioFactors **35**(2): 209-225.

Muchowski, P. J. and J. L. Wacker (2005). "Modulation of neurodegeneration by molecular chaperones." Nat Rev Neurosci **6**(1): 11-22.

Myhill, N., E. M. Lynes, J. A. Nanji, A. D. Blagoveshchenskaya, H. Fei, K. Carmine Simmen, T. J. Cooper, G. Thomas and T. Simmen (2008). "The Subcellular Distribution of Calnexin Is Mediated by PACS-2." Mol. Biol. Cell **19**(7): 2777-2788.

Nabi, I. R., G. Guay and D. Simard (1997). "AMF-R Tubules Concentrate in a Pericentriolar Microtubule Domain After MSV Transformation of Epithelial MDCK Cells." J. Histochem. Cytochem. **45**(10): 1351-1364.

Nakatsukasa and Brodsky (2008). "The Recognition and Retrotranslocation of Misfolded Proteins from the Endoplasmic Reticulum." Traffic **9**(6): 861-870.

Ni, M. and A. S. Lee (2007). "ER chaperones in mammalian development and human diseases." FEBS Letters **581**(19): 3641-3651.

Nicholls, D. G. (2008). "Oxidative Stress and Energy Crises in Neuronal Dysfunction." Annals of the New York Academy of Sciences **1147**(Mitochondria and Oxidative Stress in Neurodegenerative Disorders): 53-60.

Oliver, J. D., F. J. van der Wal, N. J. Bulleid and S. High (1997). "Interaction of the Thiol-Dependent Reductase ERp57 with Nascent Glycoproteins." Science **275**(5296): 86-88.

Otsu, M., G. Bertoli, C. Fagioli, E. Guerini-Rocco, S. Nerini-Molteni, E. Ruffato and R. Sitia (2006). "Dynamic Retention of Ero1α and Ero1β in the Endoplasmic Reticulum by Interactions with PDI and ERp44." Antioxidants & Redox Signaling **8**(3-4): 274-282.

Pagani, M., M. Fabbri, C. Benedetti, A. Fassio, S. Pilati, N. J. Bulleid, A. Cabibbo and R. Sitia (2000). "Endoplasmic Reticulum Oxidoreductin 1-Lbeta (ERO1-Lbeta), a Human Gene Induced in the Course of the Unfolded Protein Response." J. Biol. Chem. **275**(31): 23685-23692.

Pagani, M., S. Pilati, G. Bertoli, B. Valsasina and R. Sitia (2001). "The C-terminal domain of yeast Ero1p mediates membrane localization and is essential for function." FEBS Letters **508**(1): 117-120.

Parodi, A. J. (2000). "Role of N-oligosaccharide endoplasmic reticulum processing reactions in glycoprotein folding and degradation." Biochem. J. **348**(1): 1-13.

Pelham, H. R. B. (1990). "The retention signal for soluble proteins of the endoplasmic reticulum." Trends in Biochemical Sciences **15**(12): 483-486.

Pollard, M. G., K. J. Travers and J. S. Weissman (1998). "Ero1p: a novel and ubiquitous protein with an essential role in oxidative protein folding in the endoplasmic reticulum." Mol Cell **1**(2): 171-82.

Powell, K. and P. L. Zeitlin (2002). "Therapeutic approaches to repair defects in [Delta]F508 CFTR folding and cellular targeting." Advanced Drug Delivery Reviews **54**(11): 1395-1408.

Prostko, C. R., M. A. Brostrom and C. O. Brostrom (1993). "Reversible phosphorylation of eukaryotic initiation factor 2α in response to endoplasmic reticular signaling." Molecular and Cellular Biochemistry **127**(1): 255-265.

Protchenko, O., R. Rodriguez-Suarez, R. Androphy, H. Bussey and C. C. Philpott (2006). "A Screen for Genes of Heme Uptake Identifies the FLC Family Required for Import of FAD into the Endoplasmic Reticulum." J. Biol. Chem. **281**(30): 21445-21457.

Ramadan, K., R. Bruderer, F. M. Spiga, O. Popp, T. Baur, M. Gotta and H. H. Meyer (2007). "Cdc48/p97 promotes reformation of the nucleus by extracting the kinase Aurora B from chromatin." Nature **450**(7173): 1258-1262.

Riemer, J., N. Bulleid and J. M. Herrmann (2009). "Disulfide Formation in the ER and Mitochondria: Two Solutions to a Common Process." Science **324**(5932): 1284-1287.

Ron, D. and S. R. Hubbard (2008). "How IRE1 Reacts to ER Stress." Cell **132**(1): 24-26.

Schröder, M. and R. J. Kaufman (2005). "ER stress and the unfolded protein response." Mutation Research/Fundamental and Molecular Mechanisms of Mutagenesis **569**(1-2): 29-63.

Seckler, R. and R. Jaenicke (1992). "Protein folding and protein refolding." FASEB J. **6**(8): 2545-2552.

Semenza, G. L. (2000). "HIF-1: mediator of physiological and pathophysiological responses to hypoxia." J Appl Physiol **88**(4): 1474-1480.

Shen, X., K. Zhang and R. J. Kaufman (2004). "The unfolded protein response--a stress signaling pathway of the endoplasmic reticulum." Journal of Chemical Neuroanatomy **28**(1-2): 79-92.

Skulachev, V. P. (1998). "Cytochrome c in the apoptotic and antioxidant cascades." FEBS Letters **423**(3): 275-280.

So, A., E. de la Fuente, P. Walter, M. Shuman and S. Bernales (2009). "The unfolded protein response during prostate cancer development." Cancer and Metastasis Reviews **28**(1): 219-223.

Sommer, T. and E. Jarosch (2002). "BiP Binding Keeps ATF6 at Bay." Developmental Cell **3**(1): 1-2.

Szabadkai, G., K. Bianchi, P. Varnai, D. De Stefani, M. R. Wieckowski, D. Cavagna, A. I. Nagy, T. Balla and R. Rizzuto (2006). "Chaperone-mediated coupling of endoplasmic reticulum and mitochondrial Ca2+ channels." J. Cell Biol. **175**(6): 901-911.

Taylor, S. C., A. D. Ferguson, J. J. M. Bergeron and D. Y. Thomas (2004). "The ER protein folding sensor UDP-glucose glycoprotein-glucosyltransferase modifies substrates distant to local changes in glycoprotein conformation." Nat Struct Mol Biol **11**(2): 128-134.

Trombetta, E. S. and A. J. Parodi (2003). "Quality control and protein folding in the secretory pathway." Annual Review of Cell and Developmental Biology **19**: 649-676.

Tu, B. P. and J. S. Weissman (2002). "The FAD- and O2-Dependent Reaction Cycle of Ero1-Mediated Oxidative Protein Folding in the Endoplasmic Reticulum." Molecular Cell **10**(5): 983-994.

Tu, B. P. and J. S. Weissman (2004). "Oxidative protein folding in eukaryotes: mechanisms and consequences." J Cell Biol **164**(3): 341-6.

Urano, F., X. Wang, A. Bertolotti, Y. Zhang, P. Chung, H. P. Harding and D. Ron (2000). "Coupling of Stress in the ER to Activation of JNK Protein Kinases by Transmembrane Protein Kinase IRE1." Science **287**(5453): 664-666.

van Meer, G. (1989). "Lipid Traffic in Animal Cells." Annual Review of Cell Biology **5**(1): 247-275.

Vance, J. E. and D. E. Vance (1988). "Does rat liver Golgi have the capacity to synthesize phospholipids for lipoprotein secretion?" J. Biol. Chem. **263**(12): 5898-5909.

Vander Heiden, M. G., L. C. Cantley and C. B. Thompson (2009). "Understanding the Warburg Effect: The Metabolic Requirements of Cell Proliferation." Science **324**(5930): 1029-1033.

Vengellur, A. and J. J. LaPres (2004). "The Role of Hypoxia Inducible Factor 1{alpha} in Cobalt Chloride Induced Cell Death in Mouse Embryonic Fibroblasts." Toxicol. Sci. **82**(2): 638-646.

Williams, D. B. (2006). "Beyond lectins: the calnexin/calreticulin chaperone system of the endoplasmic reticulum." J Cell Sci **119**(4): 615-623.

Wong and Puthalakath (2008). "Bcl-2 family proteins: The sentinels of the mitochondrial apoptosis pathway." IUBMB Life **60**(6): 390-397.

Xie, K., D. Wei, Q. Shi and S. Huang (2004). "Constitutive and inducible expression and regulation of vascular endothelial growth factor." Cytokine & Growth Factor Reviews **15**(5): 297-324.

Yeluri, S., B. Madhok, K. Prasad, P. Quirke and D. Jayne (2009). "Cancer's craving for sugar: an opportunity for clinical exploitation." Journal of Cancer Research and Clinical Oncology **135**(7): 867-877.

Yoshida, H., K. Haze, H. Yanagi, T. Yura and K. Mori (1998). "Identification of the cis-Acting Endoplasmic Reticulum Stress Response Element Responsible for Transcriptional Induction of Mammalian Glucose-regulated Proteins. INVOLVEMENT OF BASIC LEUCINE ZIPPER TRANSCRIPTION FACTORS." J. Biol. Chem. **273**(50): 33741-33749.

Zhu, H. and H. F. Bunn (2001). "SIGNAL TRANSDUCTION: How Do Cells Sense Oxygen?" Science **292**(5516): 449-451.